

Novel Biodegradable Poly (Glycolic Acid) Dual-Layer Packaging System Using Spray
Coating

Arash (Ace) Shams

Thesis submitted to the faculty of the Virginia Polytechnic Institute and State University
in partial fulfillment of the requirements for the degree of

Master of Science
In
Forest Products

Charles E. Frazier, Chair
Robert J. Bush
Kevin J. Edgar
Maren Roman

August 4st, 2025
Blacksburg, Virginia

Keywords: Dual-Layer Packaging, Spray Coating, Poly(Glycolic Acid) (PGA),
Cellulose Nanofibrils (CNF),

Novel Biodegradable Poly (Glycolic Acid) Dual-Layer Packaging System Using Spray Coating

Arash Shams

ABSTRACT

Polymer films are essential barriers for food and consumer packaging, but because they are durable, they contribute to accumulating waste that infiltrates ecosystems, enters food chains as microplastics, and overwhelms disposal systems. This research responds by developing a biodegradable packaging system designed to reduce plastic pollution and improve environmental sustainability. A dual-layer design packaging system incorporating a cellulose nanofibril (CNF)-reinforced paper substrate spray-coated with a poly(glycolic acid) (PGA) outer layer is designed to enhance barrier performance. The approach involves spray coating CNF onto the paper substrate to effectively fill surface pores, followed by an additional spray coating of PGA to create a dense, uniform layer. This dual-layer system demonstrated notable improvements, including a substantial oxygen barrier performance to approximately $1.6 \text{ cm}^3/(\text{m}^2 \cdot 24 \text{ hour})$, improved surface smoothness, reduced roughness from $3.8 \text{ }\mu\text{m}$ to $1.3 \text{ }\mu\text{m}$, maintained good thermal stability, and enhanced hydrophobicity, with water contact angles around 60° , indicating improved moisture resistance. Scanning electron microscopy further confirmed these improvements by revealing a uniform, dense PGA coating layer with robust interfacial adhesion to the CNF-treated paper substrate. These advancements present a viable biodegradable packaging alternative aligned with circular economic principles, offering opportunities for industrial implementation.

Novel Biodegradable Poly (Glycolic Acid) Dual-Layer Packaging System Using Spray Coating

Arash Shams

GENERAL AUDIENCE ABSTRACT

Plastic waste is a growing threat to our health and the environment. Each year we produce over 400 million metric tons of plastic but recycle only about 10%. To help solve this problem using natural materials, we developed a two-layer package. First, we filled the tiny pores in paper with cellulose nanofibrils (CNF). Next, we sprayed on a thin coat of a biodegradable plastic called poly(glycolic acid) and pressed it under heat. The new films withstand temperatures above 270 °C, have smooth surfaces, are relatively more resistant to water, and allow much less oxygen to pass through. We confirmed these improvements with tests for heat stability, microscopic images, oxygen transmission, and water contact. By making packaging that breaks down naturally and can be produced in large quantities, this work supports moving away from single-use plastics and promotes a circular economy in the packaging industry.

Dedication

To my aunt Nahid, who's been telling everyone for the past 20 years that I'm a genius and should dedicate my first book to her.

I'm definitely not a genius, and I don't plan on writing a book, so I hope this will do instead.

Acknowledgments

I would like to thank Dr. Kim for having me in his lab and serving as my advisor over the past 18 months. It wasn't always smooth sailing, but I truly appreciate his patience, guidance, and encouragement throughout the process. I am especially grateful to Dr. Frazier for his support as my committee chair. His thoughtful perspective, clear feedback, and attention to detail were instrumental in shaping this thesis. I also want to thank my committee members—Dr. Bush, Dr. Edgar, and Dr. Roman—for their time, support, and valuable contributions to this work.

I am grateful to several other faculty members whose support meant a great deal during my time at Virginia Tech: Dr. Winans, Dr. Russell, and Dr. Baker. I am especially thankful to Dr. Loferski, whose kindness and generosity left a lasting impression on me.

To my lab group, Mark, JC, Atanur, Dini, Chenxi, and Zunhuang, thank you for the shared work, the conversations, and the camaraderie. I am also thankful to Mimi Harrison, Trish Colley and Maryam Kamran from the SBIO department for their steady support and countless ways of making things easier.

A special thank-you goes to Jennifer Gagnon, John Peterson, Kate Snipe and Tiffany Brown from the Department of Forestry for your guidance and generosity truly felt like being welcomed into a family.

To my friends in SBIO, Abbasali, Mona, Esra, Gurkeerat, and Collins, thank you for your support and friendship. Your presence made this experience more meaningful.

Now, to my beloved VT Friends. Majid and Bushra, Marina, Zeke, Jasmine, Fetra, Thomas, Elizabeth, Mia, Eric, Milad, Behrooz, Arezoo (Being a Fati is a privilege that you don't have, so stick with Arezoo), Masoud, Alex, Ali, Bernie, Zach, Claudia, Sinclair, Nathan, Sarah (and every other Sarah on campus, I'm still not sure how many of you there are), Will, Will, and... yes, *that* other Will (the three Wills are basically a single entity with shared brain cells), and Sami—thank you. You made life at VT unforgettable.

I would also like to acknowledge the chemistry faculty, Dr. Moore, Dr. Worch, Dr. Esker, and Dr. Morris, for their encouragement during my research.

I am sincerely grateful to the graduate school and counseling staff who supported my well-being throughout this process: Dr. Surprenant, Jeff Flanagan, Dr. Hanson, Dr. Cotrupi, Lauren Surface, Lindsay Barron, Monika Gibson and once again, Dr. Edgar. Your care and support helped me persevere.

A special thank-you to Davood Hassanian-Moghaddam and Dr. Milad Motamedi for making me feel as though I had older brothers by my side. You know how useless I am without you.

Finally, to my parents, thank you for your unwavering love and encouragement. You have been the foundation of this journey, and I owe everything to you.

Table of Contents

Acknowledgments.....	v
Table of Contents.....	vi
List of Figures.....	viii
List of Tables.....	ix
List of Abbreviations.....	x
1. General Introduction.....	1
1.1. Research Objectives and Hypothesis.....	5
2. Literature review.....	6
2.1. Multilayer Packaging.....	6
2.2. Poly (Glycolic Acid).....	7
2.3. Paper-Based Packaging.....	14
2.4. Cellulose Nanofibrils (CNF).....	19
2.5. Spray Coating.....	23
3. Experimental Materials and Procedures.....	29
3.1. Materials.....	30
3.2. Methods.....	30
3.2.1. Homogenization process.....	30
3.2.2. Preparation of Paper Layer.....	32
3.2.3. Spray Coating and Hot-Pressing CNF onto a Paper Layer.....	32
3.2.4. Preparation for PGA-Ethanol Suspension.....	33
3.2.5. Spray Coating and Hot-Pressing PGA onto Paper/CNF Layer.....	34
3.3. Characterizations.....	36
3.3.1. Thermogravimetric Analysis (TGA).....	36
3.3.2. Oxygen Transmission Rate (OTR).....	37
3.3.3. Contact Angle Analysis.....	40
3.3.4. Scanning Electron Microscopy (SEM).....	42
3.3.5. Surface Roughness Evaluation.....	45
4. Results and Discussion.....	47
4.1. Thermal Stability.....	47
4.2. Surface Roughness.....	49
4.3. Scanning Electron Microscopy (SEM).....	52
4.4. Wettability or Contact Angle.....	57
4.5. Barrier Properties.....	61

5. Conclusion.....	65
5.1. Summary of Objectives and Outcomes.....	66
5.2. Limitations	67
5.3. Recommendations for future research	68
References.....	70
Supplemental Data	79
Scanning Electron Microscopy (SEM).....	79
Surface Roughness.....	82

List of Figures

Figure 2.1. Chemical Structure of poly (glycolic acid).	8
Figure 2.2. Applications for PGA (C. Liu et al., 2024).	13
Figure 2.3. Wax-coated Pure-Pak milk carton.	15
Figure 2.4. FE-SEM micrographs of uncoated (a) and CNF-coated unbleached papers with coat weights of ca. 0.9 (b), 1.3 (c) and 1.8 g/m ² (d), respectively. The scale bar is 100 ml.	22
Figure 2.5. SEM micrograph of coated paper with nanocellulose.	26
Figure 3.1. Sample cutting workflow for OTR and other characterization tests.	29
Figure 3.2. Thermogravimetric Analysis Instrument.	37
Figure 3.3. Oxygen Transmission Rate Analysis Instrument.	38
Figure 3.4. Optical Tensiometer Instrument.	41
Figure 3.5. Scanning Electron Microscope.	44
Figure 3.6. 3D Surface profilometer Instrument.	46
Figure 4.1. Thermogravimetric weight loss profile of dual-layer packaging films under N ₂	49
Figure 4.2. Surface roughness of dual-layer packaging films: arithmetical mean height or <i>S_a</i>	51
Figure 4.3. Surface roughness of dual-layer packaging films (a) 3D and (b) z-stack images.	51
Figure 4.4. SEM surface images of dual-layer packaging samples.	54
Figure 4.5. SEM cross-sectional images showing the dual-layer packaging systems.	57
Figure 4.6. Contact angle measurements of dual-layer packaging films: (a) top surface at 0 and 60 seconds, and (b) top surface over 60 seconds.	61
Figure 4.7. Oxygen transmission rate of Paper, Paper/CNF-5, and Paper/CNF-5/PGA samples.	63

List of Tables

Table 2.1. General mechanical properties of PGA, PLA, and other polymers.....	10
Table 2.2. Degradation time of different biodegradable polymers.....	11
Table 2.3. Permeability of oxygen, carbon dioxide, and moisture of PGA, PLA, and other polymers.....	12
Table 3.1. Mean mass of samples.	35
Table 4.1. Thermogravimetric analysis of dual-Layer packaging films: Major degradation temperatures.....	49
Table 4.2. Cross-sectional thickness measurements of the whole and coated layers for each sample, obtained from SEM analysis.	56
Table 4.3. Oxygen transmission rate values of dual-layer packaging samples.	63
Table 4.4. Comparison of the oxygen transmission rate of the dual-layer sample with various polymers.	64

List of Abbreviations

PGA	Poly (Glycolic Acid)
HFIP	Hexafluoroisopropanol
PLA	Poly(lactic Acid)
PLLA	Poly-L-lactic acid
PDO	Polydioxanone
PHA	Polyhydroxyalkanoates
PCL	Polycaprolactone
PET	Polyethylene Terephthalate
HDPE	High-Density Polyethylene
PVC	Polyvinyl Chloride
EVOH	Ethylene vinyl alcohol
PE	Polyethylene
PP	Polypropylene
PS	Polystyrene
PA	Polyamide
T_d	Degradation Temperature
T_g	Glass Transition Temperature
T_c	Crystallization Temperature
T_m	Melting Temperature
WVTR	Water Vapor Transmission Rate
OTR	Oxygen Transmission Rate
TGA	Thermogravimetric analysis
SEM	Scanning Electron Microscopy
CNF	Cellulose Nanofibrils
CNC	Cellulose Nanocrystals
DCM	Dichloromethane
HPLC	High-Performance Liquid Chromatography
PTFE	Polytetrafluoroethylene
γ	Surface Tension
γ_{lv}	Liquid-Vapor Surface Tension
γ_{sl}	Solid-Liquid Surface Tension
γ_{sv}	Solid-Vapor Surface Tension
S_a	Arithmetical Mean Height Over an Entire Surface Area
ASTM	American Society for Testing and Materials
$T_{d5\%}$	Temperature at 5% Weight Loss
T_f	Final Degradation Temperature
TEC	Triethyl Citrate
FTIR	Fourier Transform Infrared Spectroscopy
S_a	Arithmetic Mean Height
PBS	Phosphate-Buffered Saline
SEC	Size-Exclusion Chromatography
STP	Standard Temperature and Pressure

CHAPTER 1

1. General Introduction

In the last half-decade, the plastics dilemma has continued to build up, raising pressing concerns about its effects on the natural environment and human health. Global plastic production today exceeds 400 million metric tons every year, much of which is not recycled appropriately and results in extensive pollution of terrestrial and marine ecosystems (Borrelle et al., 2020). Microplastic fibers persist in aquatic ecosystems and pose growing risks to biodiversity and human health (Fernandez & Trasande, 2024). Despite advances in production volumes, waste management, and recycling systems, they have remained inadequate to counter the scale and complexity of plastic pollution. This crisis should be tackled through a concerted global effort that reins in excessive production among industrialized nations while simultaneously strengthening waste control mechanisms in developing economies. Ninety- five percent of the plastics packaging material valued between \$80 and \$120 billion annually, is lost after one use packaging plastics do have numerous beneficial qualities, such as extending food shelf life and lowering emissions during transportation due to its lightweight nature (De Smet, 2016; Hasselbalch, 2025). Due to poor waste management infrastructure, especially in developing countries, much of this packaging plastics ends up in landfills or the environment, with less than half even collected for recycling (Hasselbalch, 2025; Ncube et al., 2021). It is estimated that about 8 million metric tons of plastic enter the ocean annually, which is equivalent to one trash truck every minute. With current trends, this figure can possibly double by 2030 and triple by 2050. It is estimated that by 2025, the ocean will have one ton of plastic for every three tons of fish, with plastic exceeding the entire weight of all marine animals by 2050 (De

Smet, 2016). Over 90% of plastics are petroleum-based, and this industry presently comprises 6% global oil consumption; expected to reach 20% by the year 2050 if trends continue (De Smet, 2016). It is estimated that the demand for food resources will increase by 50% by the year 2050, in accordance with projections that estimate the world will be populated by approximately 7.9 billion individuals, whereas the packaging industry is expected to expand at a rate of 12% annually. Shifts in consumption patterns in conjunction with industrial expansion in the developing world are key determinants since both heighten pressure on environmental systems and concurrently boost the demand for packaging material (Ncube et al., 2021). Therefore, governments have introduced policies favoring bio-based and renewable resources for packaging based on their role in facilitating sustainability in the food sector (Beswick & Dunn, 2002). In the face of such environmental and economic imperatives, the packaging sector is turning to sustainable options that can possibly minimize plastic waste without sacrificing functionality.

The shift from traditional plastic packaging to eco-friendly alternatives has attracted significant interest owing to the environmental issues linked to plastic litter. One of the biodegradable packaging materials, multilayer packaging that combines paper and biopolymers, is a possible alternative. Packaging serves a very important function in safeguarding products from environmental influences, preserving shelf life, and ensuring secure transportation (Wang et al., 2020). Although synthetic polymers such as polyethylene terephthalate (PET) and high-density polyethylene (HDPE) typically deliver higher tensile strength (50 to 80 MPa) and Young's modulus (1 to 2 GPa), which allow thinner and more durable films, greater flexibility (elongation at break often exceeding 200 percent), and much lower gas and moisture permeability (oxygen transmission rates below

$5 \text{ cm}^3 \cdot \text{m}^{-2} \cdot \text{day}^{-1}$ and water vapor transmission rates under $2 \text{ g} \cdot \text{m}^{-2} \cdot \text{day}^{-1}$), their perpetual presence in the environment over the long term has triggered research into biodegradable alternatives (Schmidt et al., 2022; Wang et al., 2020). Multilayer packaging structures, commonly employed in food and pharmaceutical applications, integrate various materials to perform more effectively. Their recyclability, however, poses a significant challenge because of the blending of incompatible polymers (Tamizhdurai et al., 2024). Contemporary packaging must meet sophisticated consumer needs like longer shelf life, safety assurances, and environmental sustainability pledges (Rosenboom et al., 2022). This has pushed the industry away from traditional linear models and toward circular design models that emphasize maintaining resources, minimizing emissions, and limiting solid waste production. Paper-based packaging is ubiquitous owing to its renewability and biodegradability. But the hydrophilicity of the material restricts its barrier characteristics, and it is prone to moisture uptake and eventual mechanical strength loss (Eslami & Mekonnen, 2023). To alleviate this, petroleum-based polymer or biodegradable variant coatings are used. Biopolymer coatings derived from starch, chitosan, and cellulose nanofibrils (CNF) have also shown promise in enhancing moisture resistance without compromising biodegradability (Hernández-García et al., 2022). Cellulose nanofibrils (CNF) improve significantly both mechanical strength and oxygen barrier properties and thus are a rich component in paper-based packaging material (Vartiainen et al., 2015). Poly (glycolic acid) (PGA) has been developed as an improved biodegradable polymer by virtue of its good gas barrier properties and quick degradation in natural environments (Regubalan et al., 2022). PGA exhibits superior oxygen and moisture barrier performance compared to conventional bioplastics such as polylactic acid (PLA), making it a very

promising material for the packaging of food and drugs (Cui et al., 2025). However, the highly crystalline nature of PGA and its thermal degradation issues demand processing methods that ensure well-controlled deposition and adhesion (Samantaray et al., 2020). Spray coating might be a suitable and scalable technique for PGA deposition onto paper substrates. The method enables controlled deposition, with homogeneous thin films produced that exhibit improved adhesion (Fu & Dudley, 2021). Utilization of CNF as a pre-coating layer overcomes the porosity of the paper, improving adhesion and decreasing permeability (Borrega & Orelma, 2019). The simultaneous application of spray deposition along with hot pressing improves the mechanical and barrier performance of the multilayer system significantly (López de Dicastillo et al., 2021). Research has indicated that hot pressing improves diffusion within polymers, thereby removing micro-voids and coating uniformity (López de Dicastillo et al., 2021). In spite of all these benefits, there are a few issues associated with spray coating, which need to be overcome to facilitate practical application. The limitations encountered are material losses from overspray, controlling coating thickness problems, and those imposed by high-viscosity biopolymer solutions (Gupta et al., 2022; C. Liu et al., 2024). To effectively deal with these issues, there is a need to optimize spray parameters, employ surface modifications, and formulate bio-based solvent systems towards the enhancement of sustainability (Jahangiri et al., 2024). Continued development in processing technologies and polymer modifications will likely enhance the feasibility of spray-coated biodegradable packaging for large-scale applications. Despite significant advances in creating biodegradable packaging, significant challenges persist in achieving consistent coating and ensuring scalability.

1.1. Research Objectives and Hypothesis

Hypothesis

A dual-layer structure combining polyglycolic acid (PGA) with cellulose nanofibrils (CNF) filled paper, fabricated via spray-coating, will exhibit superior barrier and thermal properties compared to conventional single-layer paper packaging.

Objectives

- Formulate a stable PGA–ethanol suspension suitable for spray-coating application.
- Establish a PGA–paper dual-layer system by filling paper pores with cellulose nanofibrils (CNF) as an interfacial bridge and depositing a uniform PGA layer over the CNF-treated paper
- Prepare dual-layer specimens under constant conditions (temperature, pressure, dwell time) and fixed CNF/PGA loadings.
- Characterize the resulting films via:
 - Thermogravimetric analysis (TGA) for thermal stability
 - Scanning electron microscopy (SEM) for morphology
 - Oxygen transmission rate (OTR) testing for barrier performance
 - Contact angle measurement for surface hydrophobicity
 - Surface roughness evaluation for coating uniformity

Expected Outcomes

Development of a hydrophobic packaging system with enhanced thermal stability, improved surface smoothness, and markedly reduced oxygen permeability.

CHAPTER 2

2. Literature review

2.1. Multilayer Packaging

Multilayer packaging has emerged as a key development in the packaging industry, such as food packaging, through the application of a blend of a number of materials, where each is selected based on its functional attributes. In comparison to single-layer packaging, which may fail to satisfy all food preservation requirements, multilayer structures integrate diverse polymeric and non-polymeric layers for enhanced barrier performance, mechanical strength, and shelf life (Schmidt et al., 2022). This approach enables packaging to provide enhanced protection from oxygen, moisture, light, and contaminants with flexibility, low cost, and light weight (Tamizhdurai et al., 2024). The primary advantage of multilayer packaging is its ability to extend product shelf life by reducing gas permeability. As noted, exposure to oxygen leads to spoilage, resulting in quality degradation of food and pharmaceutical products. This is especially useful for perishable items, including dairy, meat, and processed food, where an even internal environment needs to be sustained (Alias et al., 2022). However, despite its benefits, multilayer packaging raises environmental concerns based on its material complexity. The heterogeneity of multilayer films makes them difficult to recycle through traditional methods (Schmidt et al., 2022).

Although the benefits of multilayer packaging are evident, their structures often combine incompatible polymers, making separation and recycling difficult. Techniques like delamination and compatibilizers have been proposed to address this, but both remain limited by high cost, energy demand, and infrastructure requirements (Schmidt et al., 2022; Tamizhdurai et al., 2024).

The second limitation is the economic limitations of multilayer packaging. Barrier films with high performance extend product life and minimize food losses but are expensive to produce due to the use of sophisticated manufacturing processes, e.g., coextrusion, lamination, and coating processes. To combat these drawbacks, researchers are working on hybrid strategies involving the blending of biodegradable polymers with various sustainable approaches (Anukiruthika et al., 2020). Bio-based or biodegradable layer combinations have been a suitable alternative, with high potential. However, the majority of biodegradable films lack mechanical and moisture barrier properties necessary for large-scale application (Alias et al., 2022). Addressing the technical and environmental limitations of multilayer packaging involves moving towards circular economy principles where designing materials for recyclability is prioritized alongside technical development for the creation of eco-friendly substitutes. Novel strategies, including the development of single-material multilayer films and enzymatic recycling processes, are being explored to address the challenges of incompatibility and waste accumulation (Schmidt et al., 2022). Nonetheless, imparting large-scale sustainability to multilayer packaging is a multifaceted task that demands synergy among industry stakeholders, regulatory agencies, and scientific communities (Tamizhdurai et al., 2024).

2.2. Poly (Glycolic Acid)

PGA is a biodegradable aliphatic polyester (Figure 2.1) with increasing significance in industrial and biomedical applications due to its environmentally friendly profile and high degradation rate (Cui et al., 2025; Low et al., 2020; D. Niu et al., 2023; Peng et al., 2025). It is the simplest linear polyester, composed of repeating glycolic acid units. It has been widely recognized for its ability to degrade into low-toxic byproducts

such as carbon dioxide and water in both natural and biological environments (C. Liu et al., 2024; Regubalan et al., 2022; Wei et al., 2022). The quick non-enzymatic hydrolysis of PGA, which can happen in months, sets it apart from other biodegradable polymers like PLA and polyhydroxyalkanoates (PHA) (Du et al., 2025; Regubalan et al., 2022). PGA illustrates an extraordinary amalgamation of mechanical, chemical, thermal, and physical properties, which renders it an extremely valuable polymer in biomedical, packaging, and industrial applications. Being the simplest linear aliphatic polyester, PGA has a high level of crystallinity, outstanding barrier characteristics, and enhanced mechanical strength relative to numerous other biodegradable polymers (Regubalan et al., 2022). However, its rapid degradation in aqueous environments and brittleness pose challenges, leading to extensive research on modification strategies (C. Liu et al., 2024; Wei et al., 2022).

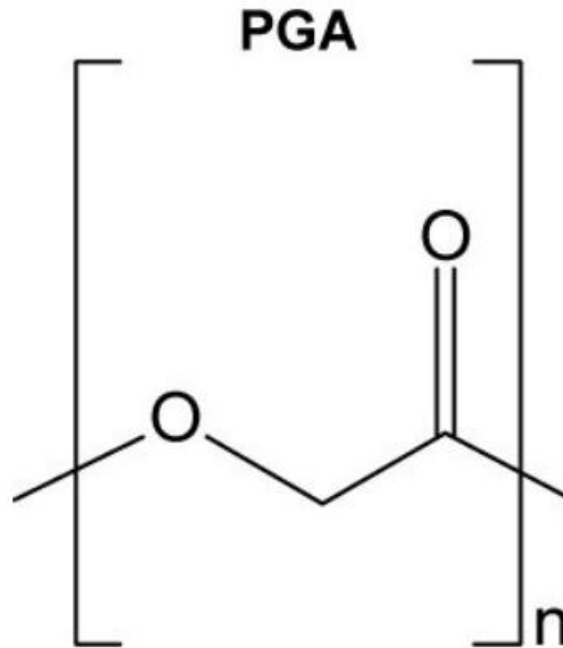


Figure 2.1. Chemical Structure of poly (glycolic acid).

The crystallinity of PGA typically ranges between 45% and 55%, significantly influencing its mechanical and thermal behavior. The polymer's molecular chains are

closely packed, forming an ordered structure that enhances rigidity and strength while contributing to its exceptional barrier properties against gas and moisture. This high crystallinity also results in a relatively high density of 1.69 g/cm^3 , which is greater than many other biodegradable polymers (Budak et al., 2020; Du et al., 2025; C. Liu et al., 2024; Morita et al., 2018; Wei et al., 2022).

Due to this compact molecular arrangement, only highly fluorinated solvents, like hexafluoroisopropanol (HFIP), can dissolve PGA. HFIP has the most significant capacity to dissolve PGA among fluoruous solvents, up to a molar mass of 45,000 g/mol. The HFIP molecule contains two potent electron-withdrawing trifluoromethyl ($-\text{CF}_3$) groups, and PGA has a significant hydrogen bond-donating capacity, accounting for its exceptional HFIP solubility. The hydrogen bonds provided by the $-\text{OH}$ group in the HFIP molecules can efficiently break or replace these weak intermolecular hydrogen interactions. (Low et al., 2020). PGA has a melting temperature (T_m) of approximately $220 - 230 \text{ }^\circ\text{C}$, significantly higher than that of PLA ($140 - 180 \text{ }^\circ\text{C}$), making it more thermally stable in certain processing conditions. The glass transition temperature (T_g) of PGA is relatively low, around $35 - 40 \text{ }^\circ\text{C}$, meaning that it can become more flexible at body temperature, which is an advantage in biomedical applications. The crystallization temperature (T_c) typically ranges from 180 to $200 \text{ }^\circ\text{C}$, enabling PGA to solidify rapidly upon cooling, enhancing mechanical strength (Cui et al., 2025; Low et al., 2020; Samantaray et al., 2020). However, PGA's thermal degradation temperature (T_d) is approximately $250 - 260 \text{ }^\circ\text{C}$, only $30-40 \text{ }^\circ\text{C}$ above its melting temperature, creating significant challenges for processing due to its narrow thermal stability window, high crystallinity, and sensitivity to hydrolytic degradation (Ma et al., 2025; Samantaray et al., 2020).

Table 2.1. General mechanical properties of PGA, PLA, and other polymers (Regubalan et al., 2022).

Material	T_m (°C)	Flexural Strength (Mpa)	Young's Modulus (Gpa)	Tensile Strength (Mpa)
PGA	220-230	222	7	115
PLA	140-180	92	2.4	53
Polyamide 6 (nylon-6)	220	77.2	2	56-90
Polystyrene (PS)	105-110	70	3-3.5	45
Polypropylene (PP)	175	40	1.5-2	31
Polyethylene Terephthalate (PET)	255	118	3.5	47

Mechanically, PGA is one of the strongest biodegradable polymers, exhibiting a tensile strength of up to 115 MPa, which is significantly higher than PLA and many conventional biopolymers, according to Table 2.1 (Regubalan et al., 2022). Its elastic modulus ranges from 6 to 7 GPa, giving it superior stiffness and load-bearing capacity. The chemical properties of PGA also play a crucial role in its performance. Beyond its impressive physical and mechanical attributes, the chemical properties of PGA, particularly its reactivity and degradation behavior, are equally critical to its functionality and application potential (Regubalan et al., 2022). The degradation mechanism of PGA is primarily driven by the hydrolysis of its ester bonds, with the amorphous regions degrading first, followed by the crystalline domains. This rapid degradation profile is advantageous for applications requiring short-term functionality, such as absorbable sutures, but presents difficulties in applications where more extended durability is needed

(Budak et al., 2020; Low et al., 2020; Samantaray et al., 2020). Table 2.2 compares the degradation times of several neat biodegradable homopolymers measured under identical *in vitro* hydrolysis conditions. For each material, preweighed specimens were immersed in phosphate-buffered saline (PBS) at pH 7.4 and 37 °C. At fixed intervals, samples were removed, rinsed, dried, and analyzed for mass loss by gravimetry and molecular-weight decline by size-exclusion chromatography (SEC) (Gentile et al., 2014; Middleton & Tipton, 2000).

Table 2.2. Degradation time of different biodegradable polymers (Regubalan et al., 2022).

Material	Degradation time (months)
PGA	1.5-3
Polycaprolactone (PCL)	24≤
Poly-L-lactic acid (PLLA)	6-24
Polydioxanone (PDO)	6-12

One of the most significant characteristics of PGA is its gas barrier properties, which are greater than those of most traditional plastics. The oxygen barrier qualities of PGA are over 1,000 times greater than PLA and approximately 100 times greater than PET. In addition, PGA also possesses excellent moisture barrier properties with a water vapor transmission rate nearly 40 times lower than that of PLA and 2–5 times lower than that of PET, as indicated in Table 2.3. Such excellent barrier properties render it highly suitable for packaging applications involving food and beverages where shelf life is a consideration. Nonetheless, as the chemical nature of PGA facilitates its distinctive degradation profile, it also presents a set of constraints in the form of brittleness and fast

hydrolysis that limit its application within certain contexts (Regubalan et al., 2022; Vartiainen et al., 2016). Despite these drawbacks, active research in the modification of polymers, copolymerization, and preparation of composites seeks to improve their performance for more general industrial use. In order to fully utilize PGA's properties and address its processing issues, PGA's preparation through various polymerization pathways has been thoroughly investigated, yielding methods for tailoring its molecular structure for specific applications (Cui et al., 2025; C. Liu et al., 2024).

Table 2.3. Permeability of oxygen, carbon dioxide, and moisture of PGA, PLA, and other polymers (Regubalan et al., 2022).

Material	Oxygen Permeability¹	Moisture vapor Permeability²	CO₂ Permeability¹
PGA	0.036	0.5	0.19
PLA	38-42	18-22	183-200
High-Density Polyethylene (HDPE)	130-185	0.3-0.4	400-700
PP	150-800	0.5-0.7	150-650
PA	2-3	16-23	10-12
PET	3-6	1-2.8	15-25
Polyvinyl Chloride (PVC)	4-30	1-5	4-50
Ethylene vinyl alcohol (EVOH)	2-2.6	1.4-6.5	N/A

¹ cm³·mil/(100 in²·day·atm)

² g·mil/(100 in²·day·atm)

Note: For O₂ or CO₂ permeability unit, is volume of gas at standard temperature and pressure. mil is specimen thickness normalization equal to 0.001 inch. 100 in² is the reference test area. day is the measurement time. atm is the applied pressure difference. For moisture vapor permeability, g is mass of water vapor. mil is specimen thickness normalization equal to 0.001 inch. 100 in² is the reference test area. day is the measurement time, and atm is the applied vapor pressure difference.

PGA was first presented as a biomaterial for medical applications. The biomedical field remains the largest consumer of PGA, using it mainly in absorbable sutures, drug delivery systems, and tissue engineering scaffolds. PGA-based sutures were the first synthetic absorbable sutures to find application in the medical field on the basis of their biocompatibility and controlled biodegradability (Ma et al., 2025; Ma et al., 2012). For

drug delivery, PGA is a biodegradable carrier for controlled release preparations with controllable hydrolysis rate through copolymerization (Cui et al., 2025; Schmidt et al., 2014). In tissue engineering, scaffolds of PGA provide temporary structure for cell growth that breaks down over time as natural tissues are formed. The aforementioned biomedical applications exploit the capacity of PGA to break down into low-toxic products, hence rendering it an excellent material for *in vivo* uses (Du et al., 2025; Low et al., 2020; D.-Y. Niu et al., 2023).

In agriculture, PGA has been investigated for possible application in biodegradable mulching films and controlled-release fertilizers (Cui et al., 2025; Samantaray et al., 2020). Conventional plastic mulch films, typically PE, significantly contribute to soil pollution as they are non-biodegradable. PGA mulch films fully biodegrade in soil within a few months without the need for removal and disposal (Du et al., 2025). Similarly, PGA has also found use in controlled-release fertilizer coatings, where its hydrolytic degradation promotes slow release of nutrients to the soil, improving crop efficiency without amplifying environmental disturbance (Regubalan et al., 2022).



Figure 2.2. Applications for PGA (C. Liu et al., 2024).

PGA has emerged as a promising food and beverage packaging material. As mentioned earlier, PGA films provide barrier properties significantly superior to other bioplastics, making them ideal for extending the shelf life of perishable foods and beverages (Cui et al., 2025; Wolf et al., 2010). In composite packaging, PGA is often used in multilayer structures where it serves as the functional high-barrier layer in combination with bioplastics (Tang et al., 2015; Vartiainen et al., 2016). Nevertheless, its moisture sensitivity advancements in surface coatings and polymer blends have improved PGA's water resistance, making it more suitable for commercial packaging applications (Morita et al., 2018).

As the global packaging industry shifts toward sustainability, PGA is expected to play an increasingly important role in developing biodegradable and high-barrier packaging solutions (Liu et al., 2025). With improved moisture resistance, processing techniques, and cost reduction, PGA-based packaging materials can replace traditional plastic packaging, contributing to a more sustainable and circular economy (Samantaray et al., 2020).

2.3. Paper-Based Packaging

Paper has long been utilized in packaging due to its renewability, biodegradability, and recyclability, making it a sustainable alternative to plastic-based materials. The fundamental component of paper is cellulose fibers, which are derived from plant sources such as wood pulp, agricultural residues, and non-wood plants. These fibers create an interwoven porous structure that provides mechanical strength, flexibility, and breathability, allowing paper to function effectively in various industrial applications.

Unlike petroleum-based polymers, paper naturally degrades in the environment, reducing waste accumulation and aligning with circular economic principles.

In spite of benefits like printability, recyclability, and visual attractiveness to the environment, paper packaging possesses weak barrier properties against moisture, grease, and oxygen, and hence its functionality is limited compared to man-made equivalents. Such drawbacks have motivated coating technology developments to enhance the functional properties of paper and widen its industrial usage (Nerín & Asensio, 2007; Rhim et al., 2006). Paper's hydrophilic nature makes it susceptible to moisture absorption, which weakens its mechanical strength. To address this, it is often modified through coatings, laminations, and structural reinforcements that enhance water resistance, grease proofing, and overall barrier performance, as seen in applications like milk packaging shown in Figure 2.3 (Eslami & Mekonnen, 2023; Tanpichai et al., 2022).



Figure 2.3. Wax-coated Pure-Pak milk carton (Twede et al., 2014).

Mulberry fiber paper is highly advantageous for sustainable and biodegradable packaging applications due to its distinctive mechanical, structural, and environmental attributes. Its exceptionally long fibers form a dense and interwoven network, granting it superior tensile strength, tear resistance, and wet stability compared to conventional wood-pulp paper (Seo & Hwang, 2019). The inherently porous yet robust fiber structure of mulberry paper provides an ideal substrate for coating processes, such as spray coating of biopolymers, by promoting strong interfacial adhesion and compatibility with advanced dual-layer packaging systems. Moreover, mulberry fiber paper is fully biodegradable, produced from renewable resources with minimal chemical processing, and environmentally benign, aligning perfectly with circular economy principles (Memon et al., 2011). These combined characteristics position mulberry fiber paper as an exceptional base material for next-generation sustainable packaging that effectively balances mechanical performance, barrier properties, and ecological responsibility.

Coatings alter the surface characteristics of paper by forming a protective film that improves its barrier performance against external forces. Surface adhesion, molecular interaction, and penetration depth of coating are the factors that determine how coatings function on paper. Mechanical adhesion is the most prevailing mechanism, in which the coating material enters the porous cellulose matrix and hardens when evaporation takes place. This mechanism finds extensive application in polymer coatings, which are water-resistant and grease-resistant (Hernández-García et al., 2022; Jahangiri et al., 2024). Conventional coating processes, such as spray coating, enable the even deposition of materials. Sophisticated techniques like extrusion coating and hot-melt application improve film formation-related characteristics. Solution-based processes, such as dip

coating and bar coating, for bio-based coating provide uniform distribution with the retention of biodegradability. Further coating technology development is required in order to increase the application of coated paper and, in this way, render it competitive with plastic packaging in end uses where enhanced barrier properties are needed (Eslami & Mekonnen, 2023; Rhim et al., 2006). Among the various techniques, spray coating delivers rapid, thin-film deposition directly onto the paper surface and is readily integrated into roll-to-roll systems, though it can suffer from material overspray and becomes challenging when using high-viscosity biopolymer suspensions (Hernández-García et al., 2022; Jahangiri et al., 2024). In contrast, extrusion coating and hot-melt processes afford solvent-free, high-throughput lamination ideal for thermoplastic polymers, but the required temperatures may degrade heat-sensitive bio-coatings (Rhim et al., 2006). Solution-based methods such as dip coating and bar (knife) coating offer uniform coverage on simple geometries with minimal equipment needs yet impose long drying times and struggle with textured or complex substrates (Eslami & Mekonnen, 2023; Rhim et al., 2006). Finally, advanced layer-by-layer assembly enables nanometer-scale control and tailored functionality, but its multistep adsorption cycles hinder throughput and scalability outside the laboratory (Tanpichai et al., 2022). Coatings for paper packaging can be generally divided into synthetic polymer coatings and bio-based biodegradable coatings, which have their respective benefits and drawbacks. These oil-based coatings, such as PE, PP, and PET, possess water and grease barrier characteristics, and they are approved for food packaging use. Their non-biodegradable qualities and the resultant recycling problems pose severe environmental concerns and increasingly restrict their use in single-use packaging. While their moisture barrier and mechanical properties are excellent, these

coatings are harmful to paper recyclability and require special separation mechanisms to avoid recycling system pollution. Keeping in view the negative environmental impact of synthetic coatings, the focus of researchers has shifted towards bio-based alternatives that provide a compromise between performance and sustainability (Rhim et al., 2006; Tanpichai et al., 2022). Bio-based coatings from polysaccharides, proteins, and biodegradable polyesters provide ecologically compatible alternatives that preserve barrier functionality while ensuring environmental friendliness. Studies show that biopolymer-based coatings, such as alginate and soy protein, enhance the water resistance of packaging using paper (Rhim et al., 2006). While Rhim and colleagues showed that the use of biopolymer coatings enhances water resistance, the small scale of their experiments limits the generalizability of these results to industry conditions (Rhim et al., 2006). Chitosan-based coatings, for example, provide antimicrobial properties and oxygen resistance, making them suitable for packaging perishable food products. Starch coatings exhibit good adhesion and medium grease resistance, though their high-water sensitivity requires them to be blended with hydrophobic biopolymers for performance optimization. PHAs and PLA coatings are biodegradable alternatives to synthetic polymers with medium water resistance and compostability. Nanocellulose-based coatings further exhibited excellent mechanical reinforcement and gas impermeability, enabling them to perform in high-performance barrier coatings for food, pharmaceutical, and industrial applications. The environmental and flexible nature of paper packaging prompted modifications to suit the demands of various industries (Eslami & Mekonnen, 2023; Wang et al., 2022).

The versatility of coated paper packaging has enabled it to be used extensively in industries ranging from food, pharmaceuticals, and cosmetics to logistics, where barrier

functionality and sustainability are the prime concerns. Coated paper is used in food packaging, fast food wrapping, bakery box packing, and packaging of dairy products, where moisture and grease resistance are necessary for preserving product integrity. (Hernández-García et al., 2022; Jahangiri et al., 2024). Development of multilayer coatings and functional additives is still widening the application of coated paper in various industries, rendering it a viable sustainable substitute for traditional plastic packaging (Eslami & Mekonnen, 2023; Wang et al., 2022). Nonetheless, with the growing application of coated paper packaging, several issues arise, most prominently the provision of cost-effectiveness and optimum recycling compatibility. The majority of biopolymer coatings, including starch and chitosan, possess extraordinary hydrophilicity, limiting their potential for complete water repellency. Additionally, the high production costs of biodegradable coatings such as PHAs and PLA restrict their large-scale implementation (Jahangiri et al., 2024; Moura, 2016).

2.4. Cellulose Nanofibrils (CNF)

Cellulose is a natural polymer that constitutes the main structural element of cell walls in plants, in addition to being present in some bacteria and algae. It is a polysaccharide comprised of linear β -(1,4)-D-glucopyranose units, which coalesce into highly ordered microfibrils via a dense network of hydrogen-bonding, thereby imparting high mechanical strength, crystallinity, and insolubility in most solvents (Borrega & Orelma, 2019; Fernández-Santos et al., 2022). Cellulose's hierarchical organization makes it simple to convert into nanocellulose, which is a family of nanomaterials exhibiting enhanced functional properties over bulk cellulose (Vartiainen et al., 2015). Cellulose has been established as a more environmentally friendly substitute for petroleum-based

polymers, thanks to its biodegradability, renewability, and facile chemical modification, and has been applied in numerous fields such as packaging, biomedical devices, and structural composites (Fernández-Santos et al., 2021).

Cellulose Nanofibrils (CNF) is manufactured from plant fibers through mechanical disintegration processes such as homogenization, microfluidization, and grinding. Because of its crystalline and amorphous cellulose regions, CNF has excellent film-forming properties, flexibility, and entanglement ability. Due to the fact that it possesses a high aspect ratio and clarity, CNF finds application in biodegradable packaging, coatings, and composite reinforcements (Wang et al., 2020). Together with its superior oxygen barrier properties, CNF's capacity to create robust and flexible films makes it a viable material for biodegradable packaging (Fourati et al., 2020; Lovely et al., 2025). Notwithstanding these encouraging uses, many obstacles prevent CNF from being widely used. One of CNF's main challenges is its hydrophilic nature, which leads to moisture absorption and a reduction in mechanical integrity and gas barrier properties. Researchers have explored chemical modifications, hybrid nanocomposites, and hydrophobic coatings to improve CNF's resistance to environmental moisture (Boufi et al., 2016). Additionally, CNF forms stable colloidal dispersions in aqueous media and demonstrates exceptional rheological properties. Its high aspect ratio and surface interactions among fibrils contribute to shear-thinning behavior, making CNF a valuable additive in bio-based inks, coatings, and thickeners (Lovely et al., 2025; Vartiainen et al., 2015). CNF's oxygen barrier performance is particularly beneficial for food and pharmaceutical packaging, where oxidation must be minimized. However, high humidity

can reduce its barrier properties, necessitating the use of surface modifications and hybrid materials to maintain efficiency (Borrega & Orelma, 2019).

Compared to many synthetic polymers, CNF films have shown reduced oxygen permeability, particularly at low to moderate humidity levels. Beyond its gas barrier properties, CNF enhances the mechanical strength and flexibility of biodegradable polymers, making it ideal for flexible packaging and coatings (Borrega & Orelma, 2019). In addition to its benefits in flexible packaging, CNF offers significant advantages when used in paper-based packaging materials. By adding CNF to recyclable paper-based packaging, structural integrity can be increased while still being compatible with current recycling methods (Vartiainen et al., 2015).

Using CNF as a coated filler is one way it is used in paper packaging. The quantity of fiber-to-fiber bonds created during consolidation and drying determines the paper's strength. Several variables influence this strength, including the distribution of residual stresses, sheet formation, specific bond strength, bonded area, and fiber length and strength. Improving any of these elements strengthens the paper as a whole. Paper is strengthened by CNF in two primary ways. First, it acts as an adhesion promoter by bridging adjacent fibers, increasing the bonded area, and reinforcing fiber-fiber bonding (Figure 2.4).

Second, CNF forms a fine network within the larger fiber structure, improving the paper's load-bearing capacity. Its micro-scale length enhances fiber entanglement, further expanding the bonded area. Due to the structural similarity between CNF and cellulose fibers, a potent natural affinity exists between them, leading to an additive effect on final paper strength. CNF-based packaging materials have broader issues that need to be addressed outside of their application in paper (Boufi et al., 2016).

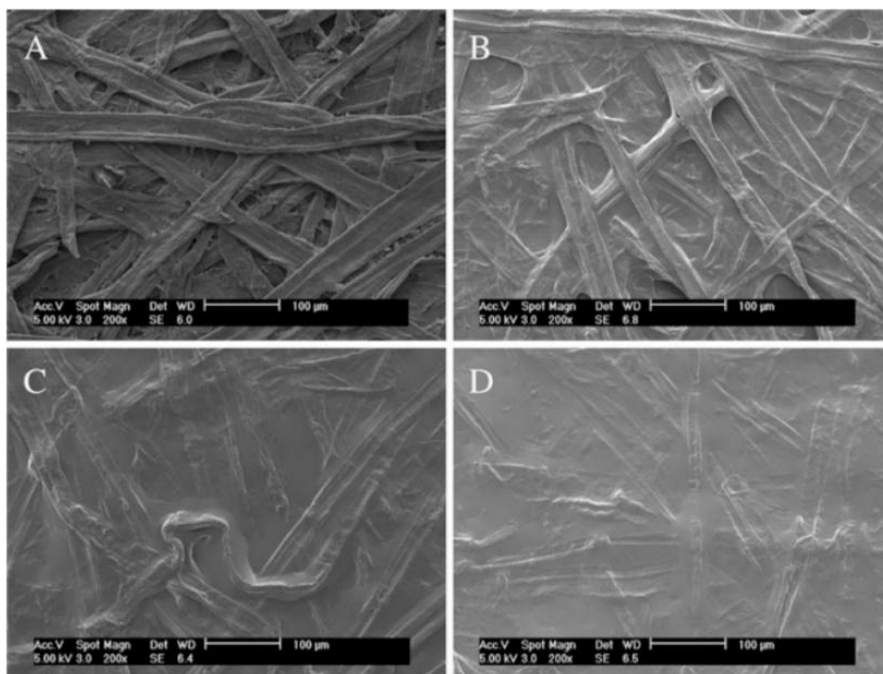


Figure 2.4. FE-SEM micrographs of uncoated (a) and CNF-coated unbleached papers with coat weights of ca. 0.9 (b), 1.3 (c) and 1.8 g/m² (d), respectively. The scale bar is 100 µm (Aulin et al., 2010).

Despite its advantages, CNF-based packaging materials face moisture sensitivity and processability challenges. Researchers have developed surface modifications, hybrid composite formulations, and multilayer structures incorporating hydrophobic coatings or cross-linked networks to address these issues and improve water resistance (Lovely et al., 2025). For example, combining CNF with wax coatings, nanoclays, or hydrophobic biopolymers has enhanced moisture resistance while preserving gas barrier efficiency. The future of CNF-based packaging lies in the continued development of scalable and cost-effective production methods that enable commercial viability. As research progresses, CNF processing and large-scale integration optimization are expected to expand its adoption in the sustainable packaging industry (Fernández-Santos et al., 2022).

In order to obtain the mentioned properties, various production techniques, such as homogenization, are employed to generate CNF from various sources (Fourati et al., 2020). Homogenization is one of the typical CNF production processes because of its

effectiveness in disintegrating cellulose fibers into nanoscale fibrils without destroying their structural integrity. Homogenization entails submitting cellulose suspensions to high mechanical forces enabling fibrillation via shear, impact, and cavitation. The degree of fibrillation and final CNF characteristics depend on significant parameters like operating pressure, number of passes, fiber concentration, and pre-treatment methods (Granda et al., 2020). Condition optimization of homogenization is key to fibrillation efficiency, energy consumption, and material property balance. By carefully controlling pressure, cycle number, fiber loading, and pre-treatment, researchers are able to obtain high-quality CNF with improved mechanical performance, stability in dispersion, and barrier function. As processing technology continues to develop, additional gains in homogenization processes will advance the scalability and economics of CNF production for biodegradable packaging, biomedical devices, and high-performance composites. Recent studies, such as the doctoral work by Dr. Lovely (Lovely, 2024), highlight advancements in CNF production that address these processing challenges. In her work, Dr. Lovely demonstrated that after 5 cycles of mild-conditioned homogenization, surface smoothness increased by 44%. At the same time, oxygen permeability decreased by 48%, enhancing the material's barrier properties. This novel low-pressure approach, using an emulsifying cell without a plasticizer, addresses significant limitations of conventional CNF processing, making it a promising alternative for applications such as oxygen-barrier packaging and UV-blocking films (Lovely et al., 2025).

2.5. Spray Coating

Researchers have extensively studied spray coating processes, emphasizing their versatility for various substrates, uniform coating application, and industrial scalability.

Spray coating is a widespread method in industry and laboratory practice that enables the controlled deposition of liquid-based coating onto substrates. The method is based on the atomization of the coating liquid into extremely tiny droplets, which are then transported to the substrate to be coated. Following deposition, the droplets merge to create a solid film. This technique is appreciated due to its scalability, affordability, and versatility for various applications, ranging from protective coatings to functionalized surfaces for food packaging (Fu & Dudley, 2021). One of the primary benefits of spray coating is that it can create homogenous films with nanoscale thickness, making it ideal for applications requiring accurate material deposition, and it is also utilized in high speed production lines (Colomer et al., 2017; Kunam et al., 2024). Nevertheless, techniques are needed to reduce the volume of spray-coating liquid and solvent used, thereby lowering cost and health risks, while maintaining processing efficacy. By taking advantage of its compatibility with less expensive and less toxic secondary solvents, solvent exchange achieves a reduction in the use of toxic solvents like HFIP. Orderly polymer precipitation is induced, and nanoparticle formation is assisted by the gradual replacement of HFIP with a solvent characterized by possessing a decreased solvating ability (Peters et al., 2025). This method has been applied in spray coating to optimize polymer solution processing, reducing operational costs and environmental impact. For instance, solvent exchange with ethanol has been effective in precipitating polymeric components without altering their morphological properties (Yoon et al., 2020). This approach is within the context of developing sustainable and scalable processing techniques in advanced polymeric coatings, particularly in packaging and biomedical applications, where stringent control of solvent removal and material deposition is required.

Spray coating is highly suitable for applications such as food packaging. Unlike conventional coating methods such as dip-coating or extrusion, spray coating does not require direct immersion of the substrate, reducing contamination risks and preserving functional characteristics of the coated material. Additionally, spray coating allows for precise control over deposition parameters, enabling the creation of high-performance coatings with tailored surface functionalities (Kunam et al., 2024). In food packaging, spray coating greatly enhances barrier functionality and mechanical strength. Spray-deposition coatings can impart moisture resistance, gas impermeability, and hydrophobic surface properties, thereby leading to extended shelf life of foods and reduced spoilage (Fu & Dudley, 2021). Another example of the utilization of this methodology in food packaging is the fabrication of layer-by-layer coatings using cationic chitin nanofibers combined with anionic cellulose nanocrystals (CNC). Such coatings have been shown to exhibit improvement in oxygen barrier properties by more than 70%, thus inhibiting the permeation of gases responsible for food spoilage. However, increasing the coating thickness beyond a certain optimum value can lead to interlayer delamination, further compromising the mechanical integrity of the film (Jahangiri et al., 2024).

Increasing demand for environmentally sustainable and biodegradable packaging materials has promoted the application of bio-based spray coatings, including nanocellulose films and chitin-based layers, with enhanced mechanical stability and environmental degradability than synthetic polymer coatings (Shanmugam, 2024). Spray coating's capability to deposit these materials positions it as a preferable method for the creation of future sustainable packaging solutions. Spray coating finds extensive use in the production of barrier coatings for packaging films made of paper and polymers. Bio-based

coatings offer a cleaner option with biodegradability and recyclability without compromising performance integrity (Jahangiri et al., 2024).

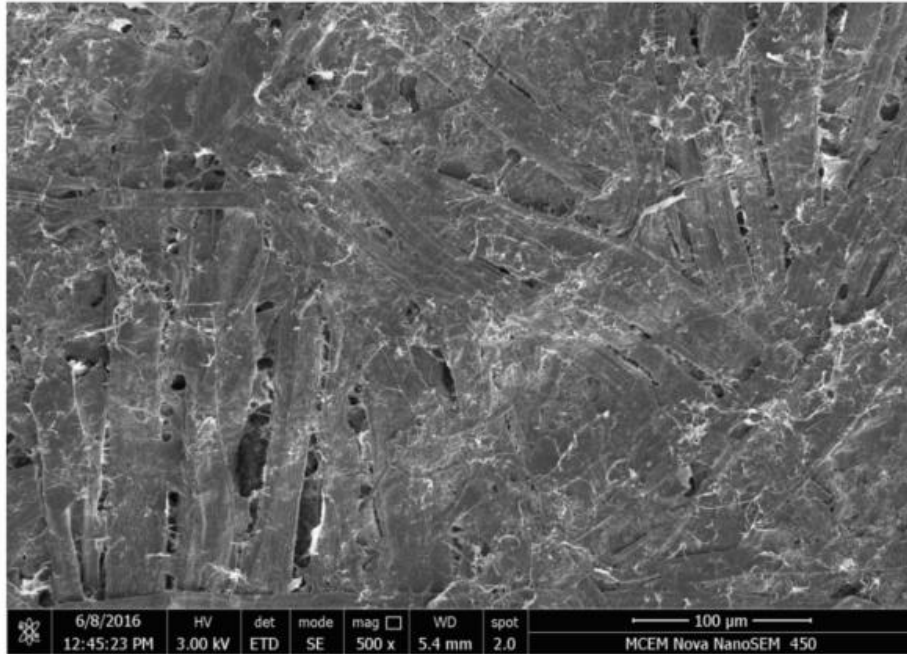


Figure 2.5. SEM micrograph of coated paper with nanocellulose (Shanmugam, 2024).

Nanocellulose-based coatings offer a green alternative to synthetic films used for food packaging. Such coatings enhance mechanical robustness, water resistance, and barrier properties by forming a dense network that slows down the diffusion of oxygen, moisture, and grease, thus improving the preservation of foods. In addition, they maintain high optical transparency, making them amenable to transparent packaging applications. Strong adhesion of nanocellulose layers to paper (see Figure 2.5) and polymeric substrates minimizes delamination risks and maximizes structural strength, a critical design factor for flexible and printed packaging uses (Shanmugam, 2024).

Despite widespread use in industrial and research applications, spray coating presents several technical and practical challenges impacting its efficiency and material performance. Issues such as material wastage due to overspray, difficulty achieving

uniform thickness, and limitations when using high-viscosity biopolymers remain significant obstacles to its broader adoption in specific applications (Gupta et al., 2022). One of the most critical challenges in spray coating is material loss due to overspray, which occurs when atomized droplets fail to reach the substrate or rebound upon impact. This inefficiency leads to increased coating material consumption, raising production costs and reducing the sustainability of the process (Kunam et al., 2024). Another major limitation of spray coating is the difficulty in controlling coating thickness. Since the deposition process relies on atomized droplets, nozzle type, spray pressure, and fluid viscosity variations can lead to uneven coatings. This issue is particularly problematic in applications requiring precise layer thickness, such as nanocoatings (Fu & Dudley, 2021). Using high-viscosity biopolymer solutions also poses a challenge, as these materials tend to clog nozzles, form non-uniform droplets, and require higher spray pressures to achieve proper atomization (Gupta et al., 2022). Additionally, spray-coated films can be susceptible to inferior adhesion on some substrates, particularly low surface energy substrates such as polyethylene (PE) and polypropylene (PP) packaging substrates. When the coating delaminates, hot pressing is omitted, or it develops compromised barrier performance due to a lack of surface treatment or primer coatings, the end product's functional properties are adversely affected (Fu & Dudley, 2021). Hot pressing has been shown to enhance the interfacial adhesion and mechanical integrity of multilayer coatings by promoting polymer infiltration into paper substrates, and molecular diffusion under high temperature and pressure. This process softens polymers, increasing their molecular mobility, which facilitates hydrogen bonding, and the formation of a continuous interface that resists delamination (Y. Liu et al., 2024; López de Dicastillo et al., 2021). It also eliminates

surface roughness and microvoids, resulting in a denser, more homogeneous structure with improved barrier properties. As a post-treatment step, hot pressing can complement spray coating, particularly in nanocellulose-based films, by minimizing coating defects and enhancing the stability and durability of biodegradable packaging (Cho et al., 2010; Rocca-Smith et al., 2019). Moreover, environmental and regulatory considerations have a significant influence on the scalability of spray coating, especially solvent-coating-based formulations. Emission of volatile organic compounds in the spray deposition process drive the need for either aqueous dispersions or solvents derived from renewable biomass that can deliver equivalent coating performance while dramatically reducing toxic emissions (Jahangiri et al., 2024). Researchers are exploring advanced spray techniques, biopolymer modifications, and sustainable solvent systems to address these challenges. While spray coating remains a highly versatile and scalable deposition method, its challenges necessitate ongoing technological improvements to enhance coating efficiency, material compatibility, and environmental sustainability. Research in advanced spray techniques, biopolymer modifications, and sustainable solvent systems continues to address these limitations, expanding the potential applications of spray coating across various industries (Y. Liu et al., 2024; López de Dicastillo et al., 2021; Vartiainen et al., 2016).

CHAPTER 3

3. Experimental Materials and Procedures

This study aimed to develop a biodegradable dual-layer packaging structure by combining poly(glycolic acid) (PGA) and paper through spray coating, with the dual goals of improving functional performance and demonstrating a viable fabrication method. Specifically, the work focused on evaluating barrier performance, hydrophobicity, and thermal stability, while also establishing a stable PGA ethanol suspension and constructing a layered structure using cellulose nanofibrils (CNF) as a pore-filling interlayer. Three sample types were prepared: Paper, Paper/CNF 5, and Paper/CNF 5/PGA, with one specimen per type. Each sample was subdivided for characterization tests, including oxygen transmission rate (OTR) analysis, scanning electron microscopy (SEM), thermogravimetric analysis (TGA), contact angle measurement, and surface roughness analysis via 3D surface profiling. The workflow for sample subdivision is illustrated in Figure 3.1.

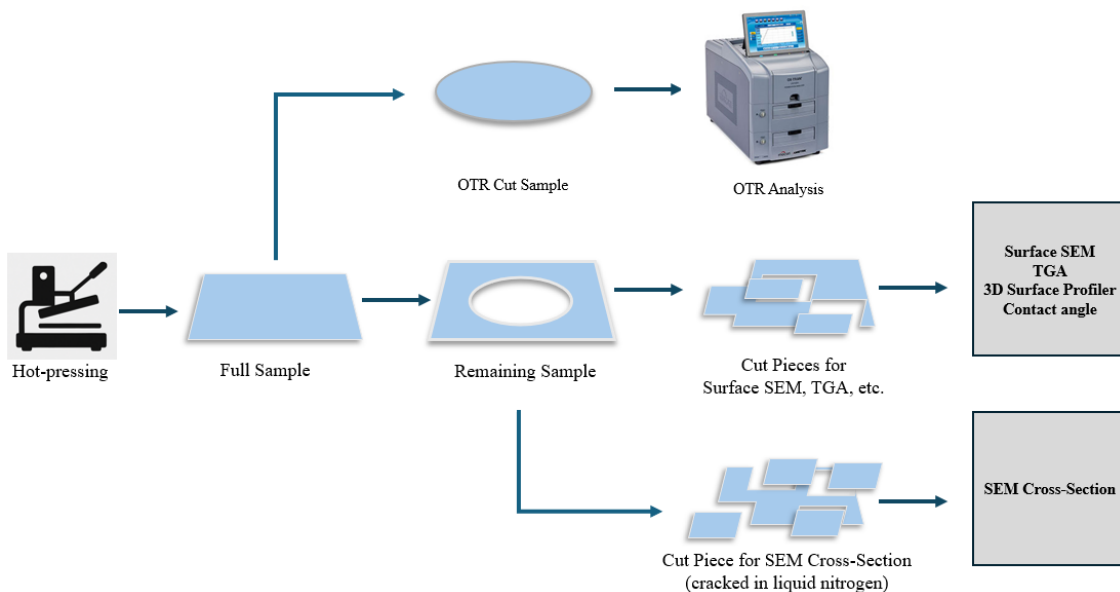


Figure 3.1. Sample cutting workflow for OTR and other characterization tests.

3.1. Materials

Mulberry fiber paper (cellulose-based), used as the first layer of the bioplastic packaging, was provided by Kyung Hee University (Seoul, South Korea). The paper layer was filled with CNF made from northern bleached softwood kraft pulp, which was acquired from the University of Maine's Process Development Center. (Orono, ME, USA). High-Performance Liquid Chromatography (HPLC) grade water for dilution and processing of CNF was purchased from EMD Millipore (Burlington, MA, USA). PGA, serving as the second layer of the bioplastic system, was supplied by LG Chem (Seoul, South Korea). HFIP, used as the primary solvent for dissolving PGA, was sourced from Sigma-Aldrich (St. Louis, MO, USA). Dichloromethane (DCM), used as a solvent in the process, was purchased from Fisher Chemical (Fair Lawn, NJ, USA), and ethanol (95%) was obtained from Decon Laboratories, Inc. (King of Prussia, PA, USA). Polytetrafluoroethylene (PTFE) Teflon sheets used during the hot-pressing steps were supplied by LJXBMD. Triethyl citrate (TEC), used as a plasticizer in the PGA coating, was sourced from Tokyo Chemical Industry Co., Ltd. (Tokyo, Japan).

3.2. Methods

3.2.1. Homogenization process

The CNF slurry, initially containing 3% solids by mass, was diluted by manually mixing 1 liter of the CNF slurry with 3 liters of HPLC-grade water (1:3 volumetric ratio). This mixture was stirred continuously in an open atmosphere for 30 minutes to ensure uniform dispersion, resulting in a neat CNF suspension with an approximate solids content of 0.75% by mass. This diluted suspension was then processed using a Mini DeBEE 30

homogenizer (BEE International, South Easton, MA, USA), equipped with a 0.20 mm (0.008 inch) nozzle. Each homogenization cycle involved pumping the suspension through the homogenizer's spring-loaded valve assembly at a conditioning pressure of approximately 7 MPa. During each cycle, the valve assembly repeatedly opened and closed, creating pressure drops that induced high shear, cavitation, and impact forces as the suspension passed through the narrow nozzle. Each pass through the homogenizer nozzle took approximately 3–5 seconds, promoting consistent and effective fibrillation, enhancing hydrogen bonding, and reinforcing the structural integrity of the resulting CNF network (Lovely et al., 2025). The suspension underwent five complete homogenization cycles, based on preliminary trials and previous studies recommending fewer than 30 passes to minimize shear damage and preserve structural integrity under medium-to-low pressure conditions (Cheng & Via, 2017; Chun et al., 2011; Li et al., 2018). After homogenization, additional HPLC-grade water, equivalent to 12% of the total homogenized suspension's mass, was added and stirred continuously at 400 rpm for another 30 minutes in a borosilicate glass storage bottle to reduce viscosity and improve sprayability. This further dilution resulted in a slight reduction of CNF solids content to approximately 0.67% by mass. The final suspension, labeled CNF-5, was subsequently used in the coating process. Throughout the homogenization procedure, temperature was carefully regulated between 10 °C and 15 °C using the homogenizer's internal cooling system in conjunction with an external Isotemp Refrigerated Circulating Bath 910 (Fisher Scientific, Waltham, MA, USA), to avoid crystallinity loss, excessive energy consumption, and nozzle clogging.

3.2.2. Preparation of Paper Layer

The handmade mulberry fiber-based paper was first cut into 127 mm × 127 mm (5 in × 5 in) sheets. The paper was then hot-pressed at 100 °C for 10 minutes under 4.14 MPa (600 psig) using a Carver Laboratory Press (Fred S. Carver Inc., Wabash, IN, USA). Stainless-steel mirror plates were cleaned with ACS-grade acetone (Greenfield Global USA Inc., Pharmco-Aaper brand, CAS No. 67-64-1) and wiped with Kimwipes® Low-Lint Wipers (Kimberly-Clark Professional) before being placed in contact with both sides of the paper. This procedure aimed to densify the paper, improving its surface smoothness and mechanical integrity, which are critical for achieving uniform coating application. The hot-pressed paper was subsequently used as the First layer of the dual-layer packaging system. After hot pressing, one paper sheet intended as the control (uncoated) paper sample was placed in a Quincy Lab Model 40GC oven (Quincy Lab Inc., USA) at 125 °C for 24 hours to remove any residual moisture. During oven storage, the relative humidity was effectively 0%, and the sample was not exposed to light. The remaining sheets were allowed to cool at room temperature for 10 to 15 minutes in an open atmosphere before being used for subsequent CNF spray coating.

3.2.3. Spray Coating and Hot-Pressing CNF onto a Paper Layer

CNF-5 suspension (60 ml) was spray-coated onto the paper surface using an Iwata Hi-Line HP-TH airbrush (Anest Iwata, Japan) with a 0.8 mm nozzle. Before reaching this step, one of the difficulties was that the homogenized CNF had high viscosity and was difficult to spray using the available equipment. That is why it was diluted after homogenization, as described earlier. After spraying, the coated samples were left to dry at room temperature in an open atmosphere for 12 hours. During this time, some shrinkage

was observed on the paper/CNF surface. Once dried, the samples were hot-pressed at 130 °C for 15 minutes under 4.14 MPa (600 psig) using a Carver Laboratory Press (Fred S. Carver Inc., Wabash, IN, USA). As in previous steps, stainless steel mirror plates, were cleaned using ACS grade acetone (Greenfield Global USA Inc., Pharmco Aaper brand, CAS No. 67 64 1) and wiped with Kimwipes® Low Lint Wipers (Kimberly Clark Professional) before being placed in contact with both surfaces of the samples during pressing. After hot pressing, the sealed pressing plates were exposed to high speed airflow from the laboratory compressed air outlet for approximately 30 seconds to accelerate cooling. The air was not applied directly to the sample surface; instead, the plates remained closed during cooling to prevent potential oil or particulate contamination from reaching the CNF layer. The samples were then stored in a Quincy Lab Model 40GC oven (Quincy Lab Inc., USA) at 125 °C for 24 hours to prevent moisture absorption.

3.2.4. Preparation for PGA-Ethanol Suspension

PGA pellets were dissolved in HFIP at 10% wt. under continuous stirring at 400 rpm and 50 °C in a closed atmosphere using a round-bottom flask for 24 hours. Solubilization was confirmed visually, and no undissolved particles were observed after this period. The resulting 100 mL of the PGA-HFIP solution was gradually added to 1 L of DCM (1:10 volumetric ratio) while stirring at room temperature for 30 minutes. Upon addition to DCM, the PGA formed a cloudy suspension, indicating the presence of fine, insoluble particles uniformly dispersed throughout the solvent. This suspension was then sonicated using a Fisherbrand CPX1800 Ultrasonic Bath (Fisher Scientific, USA) for 1 hour at a power setting of 70 W to improve dispersion. After sonication, the entire 1100 mL of PGA-HFIP/DCM suspension was added dropwise into 2200 mL of ethanol (1:2

volumetric ratio) while stirring at 400 rpm for 24 hours in a borosilicate glass bottle. during application with available airbrush. Precipitated PGA was separated using an Eppendorf 5804 Benchtop Centrifuge (Eppendorf, Germany) at 3000 rpm for 5 minutes to remove residual solvents from the mixture. Centrifugation was repeated 5 times with fresh ethanol to ensure thorough removal of solvents. The recovered PGA appeared as a damp, cake-like solid with a cohesive texture due to residual ethanol. After the final centrifugation, the wet PGA solids were transferred from centrifuge tubes to a sealed borosilicate glass storage bottle by rinsing with ethanol. The bottle was stirred at 350 rpm and room temperature for 1 hour to maintain the mixture as a suspension. The solids content of the PGA-ethanol suspension was determined to be $2.73\% \pm 0.17$ by mass, based on triplicate moisture analysis using an OHAUS MB45 Moisture Analyzer (OHAUS Corporation, USA). To measure this, 1 mL of the thoroughly stirred suspension was placed in the analyzer and dried at 105 °C until constant weight for 8 hr. The process was repeated three times to calculate the average. This PGA suspension was then stored in a borosilicate glass storage bottle at room temperature until it was used in the next step. (Johnson et al., 2021; Lettieri et al., 2025; Peters et al., 2025; Yoon et al., 2020).

3.2.5. Spray Coating and Hot-Pressing PGA onto Paper/CNF Layer

Before spray coating, the PGA suspension was stirred again at 350 rpm for 1 hour at room temperature to reestablish uniform dispersion. A volume of 12 mL of the suspension, containing approximately 0.2681 g of solid PGA, was placed into the sprayer for coating. This quantity was used for each sample. Triethyl citrate (TEC) was added at 10% by weight relative to the solid PGA as a plasticizer to improve film flexibility and reduce brittleness. Exactly 11.8 μL of TEC was added to the suspension and stirred

magnetically for 10 to 15 minutes to ensure uniform mixing. The modified suspension was then spray-coated onto the CNF-paper surface using the Iwata Hi-Line HP-TH airbrush (Anest Iwata, Japan). The coated samples were dried inside a fume hood under ambient laboratory conditions for 30 minutes. After drying, the samples were hot-pressed at 225 °C for 2 minutes under 8.27 MPa (1200 psig) using the Carver Laboratory Press (Fred S. Carver Inc., Wabash, IN, USA). PTFE Teflon sheets (LJXBMD) were placed on both sides of the sample to prevent the PGA layer from adhering to the hot-press plates. It is important to note that the temperature listed here refers to the instrument’s set value, not the actual temperature between the mirror plates. No thermocouples or internal sensors were used during pressing, so the exact temperature at the sample surface may have varied due to heat transfer limitations or material resistance, which is especially relevant given PGA’s narrow processing window. After hot pressing, the sample remained sealed between the stainless steel mirror plates, which were placed in open laboratory air for 30 seconds to cool. This allowed the PGA chains to reorganize and promote the formation of ordered crystalline regions while preventing contamination. The sample was removed from between the plates after cooling. The final samples were then stored in a Quincy Lab Model 40GC oven (Quincy Lab Inc., USA) at 125 °C for 24 hours. After oven storage, all samples were placed in a sealed desiccator containing silica gel to protect them from ambient moisture before testing. The final prepared samples (Paper, Paper/CNF-5, Paper/CNF-5/PGA) were each weighed three times, and the mean masses are summarized in Table 3.1.

Table 3.1. Mean mass of samples.

Sample	Mean Mass (g)
Paper	0.722 ± 0.009
Paper/CNF-5	0.915 ± 0.030
Paper/CNF-5/PGA	1.270 ± 0.042

3.3. Characterizations

3.3.1. Thermogravimetric Analysis (TGA)

TGA is one of the conventional thermal techniques to determine thermal stability and compositional characteristics of materials. Additionally, TGA plays a key role in establishing the degradability of materials when subjected to various environmental conditions, thus helping create sustainable and recyclable materials (Brunšek et al., 2023). Thermal degradation analysis was conducted with a TGA 550 Thermogravimetric Analyzer (TA Instruments, New Castle, DE, USA) using pyrolytic TGA (N_2), as indicated in Figure 3.2, to examine the thermal stability of the materials in a temperature range of 25 °C to 600 °C. The samples were pre-equilibrated at 30 °C before heating. A 5 mg sample was placed in the crucible and heated at a controlled rate of 5 °C per minute. The temperature at 5% weight loss ($T_{d5\%}$), and final degradation temperature (T_f) were derived from the TGA thermograms. The resulting values provide thermal changes relating to each decomposition process of the materials, providing essential data on their thermal stability. Data were analyzed with either TRIOS or TA Universal Analysis software (TA Instruments, New Castle, DE, USA).



Figure 3.2. Thermogravimetric Analysis Instrument.

3.3.2. Oxygen Transmission Rate (OTR)

Barrier properties are essential when designing materials that require protection from environmental factors such as water vapor, humidity, gases (e.g., oxygen), or temperature fluctuations. These properties help delay degradation and extend the shelf life of sensitive products. Among the key parameters, oxygen permeability determines how easily oxygen molecules penetrate a material (Ehrmann, 2024). Oxygen is one of the most studied permeants due to its ability to migrate between internal and external environments (Siracusa, 2012). Given that the molecular diameter of oxygen is 2.98×10^{-8} cm, materials with pore sizes are more significant than this threshold exhibit higher oxygen permeability. Oxygen plays a vital role in numerous degradation processes, including lipid oxidation, microorganism growth, enzymatic browning, ethylene-induced ripening, and the deterioration of organoleptic properties such as flavor, color, and nutrient content (Ayranci & Tunc, 2003; Brown, 1992; Hong & Krochta, 2006; Russo et al., 2006). Oxygen

permeability testing can be conducted under controlled relative humidity and temperature conditions, influencing the material's oxygen diffusion and solubility. Other contributing factors include cohesive energy density, polarity, crystallinity, and chemical structure, affecting the material's free volume and permeability (Atiqah et al., 2019; Miller & Krochta, 1997). The measurement principle is based on the differential pressure or concentration-driven oxygen diffusion through a sample film. The testing apparatus employs a dual-chamber system, where one chamber is supplied with oxygen or air while the other is purged with nitrogen to create a concentration gradient. A pre-conditioned film sample is mounted within the system under ambient atmospheric pressure. As oxygen permeates through the film, it is carried by the nitrogen flow into a coulometric sensor, which detects the generated electrical signals corresponding to the oxygen concentration.



Figure 3.3. Oxygen Transmission Rate Analysis Instrument.

This study measured the samples' OTR using a gas transmission-rate tester (C230, Labthink Inc., Boston, MA, USA) following American Society for Testing and Materials (ASTM) D3985 standards. The test was conducted at 23 °C with a relative humidity of 0%. Before testing, the thickness of the films was measured using a digital thickness gauge (700-118-20 Quick Mini, Mitutoyo, Kawasaki, Japan) by recording 10 random readings to the nearest 0.001 mm, and the average value was used for subsequent calculations. The film sample was then placed into the test chamber, where the "Film-ASTM" test mode without compensation was selected. The system underwent a purging process with nitrogen gas for 30 seconds between cycles to ensure gas purity. The instrument was preheated for 2 hours before testing. The test parameters were set to a flow rate of 100 mL/min, a relative humidity of 0%, and a temperature of 23 °C. Each measurement cycle begins with a 30-second purge of the downstream chamber using pure nitrogen to clear residual oxygen and establish a stable baseline. Once the sensor readout stabilizes, nitrogen flows through the downstream cell at 100 mL per minute, while oxygen flows through the upstream chamber at the same flow rate. This creates a constant concentration gradient across the film sample. As oxygen molecules diffuse through the specimen, they combine with the nitrogen stream and pass through the coulometric detector, which continuously records the electrical signal for 30 minutes. After each interval, the instrument automatically rezeroes, and the cycle repeats. Five consecutive cycles are performed on the same specimen, and the final OTR is calculated by averaging these 5 measurements. This entire process was repeated 3 times for each specimen to confirm data consistency. Thus, the reported OTR values represent the average obtained from 3 replicates of the same specimen, with each replicate undergoing 5 test cycles.

3.3.3. Contact Angle Analysis

Surface wettability, i.e., hydrophilicity or hydrophobicity, is a crucial property that indicates the solid-liquid interface and intermolecular forces of a material. It is intrinsically connected with surface energy, adhesion force, wetting, and absorption behavior, and thus acts as a crucial parameter in material evaluation (Good, 1992; Pauleau, 2006). Wetting behavior can be generally described as the tendency of a liquid to spread across or to form discrete droplets on a solid surface and is governed by intermolecular forces. Contact angle measurements are usually conducted in an optical tensiometer, also referred to as a drop-shape analyzer or goniometer. In this approach, a dropper dispenses the test liquid on the surface of the sample as a camera, in association with an LED light source, continuously illuminates and records the behavior of the droplet in real-time. A three-phase contact line forms at the solid, liquid, and vapor interface, marking the surface tension (γ) between the liquid-vapor (γ_{lv}), solid-liquid (γ_{sl}), and solid-vapor (γ_{sv}) phases. The interfacial tensions are calculated using the Young–Laplace equation, affording the contact angle of the sample. Based on the wettability classification, a material with a contact angle of $< 90^\circ$ is hydrophilic, and a material with a contact angle of $> 90^\circ$ is hydrophobic (Del Rio & Neumann, 1997; Khan et al., 2019; Zhang et al., 2023). Contact angle measurement is widely regarded as one of the simplest, most cost-effective, and most reproducible methods for evaluating surface wettability (Cobb et al., 2018; Yang et al., 2019).

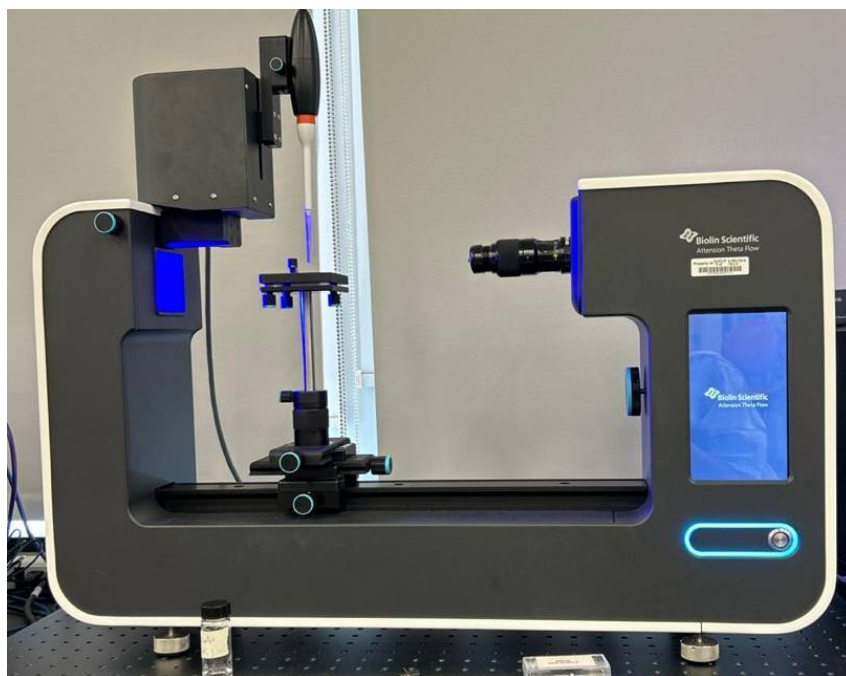


Figure 3.4. Optical Tensiometer Instrument.

Water contact angle (WCA) measurements were performed in this study using a Theta Flow contact-angle goniometer (Biolin Scientific Inc., Linthicum Heights, MD, USA) presented in Figure 3.4. The sessile drop method was employed, in which a 5 μL droplet of HPLC-grade water was carefully deposited onto the sample surface using a 200 μL pipette tip at a controlled dispenser speed of 25 $\mu\text{L}/\text{min}$. Contact angles were measured by the $\theta/2$ method, which fits a circle to the droplet profile and defines the contact angle as half of the apex angle at the liquid–solid interface. The camera began recording at the moment the drop touched the surface, so the first frame ($t = 0$ s) captures the initial contact angle. The optical system was configured with light and heavy phases (air and water at 20 $^{\circ}\text{C}$) to account for density differences in surface tension calculations. Images were recorded automatically at roughly 0.6 s intervals for a total of 60 s, yielding a high-resolution time series of contact angles from the same drop on each film. For each film, contact angles at

0 s and 60 s were extracted from that single sessile-drop sequence, capturing the change in wetting behavior over time without additional replicate droplets.

3.3.4. Scanning Electron Microscopy (SEM)

Morphological analysis offers key information regarding the structural organization and molecular arrangement of materials, ranging from the nanoscale level (e.g., crystalline lamellae and nanoparticles) to the macroscale level (e.g., mechanical and surface properties). The morphology is influenced by a variety of parameters such as molecular weight, branching, crosslinking, and crystallinity, and influences the mechanical, chemical, electrical, thermal, adhesive, and wettability performance of the material (Araki et al., 1998; Khalifeh, 2020). Morphological characterization may be accomplished using direct or indirect methods, with direct observation enabled by various microscopic techniques, which vary in resolution and magnification (Maxfield, 1994). Among these methods, electron microscopy is generally favored over optical microscopy because of its superior resolution capabilities. Although optical microscopy is considered to be cost-effective and non-invasive, it is hampered by the wavelength of visible light (400–700 nm); however, electron microscopy uses shorter wavelengths and, as such, achieves higher resolution (Spence, 2013). Electron acceleration and momentum, which are determined by applied voltage, also affect the image quality (Reimer, 2000; Vinet & Zhedanov, 2011). The negatively charged electrons produce intense interactions with atomic structures, allowing for high-resolution imaging even of nanomaterials below 15 nm. SEM is a robust electron microscopy method mostly utilized for surface morphology characterization. In contrast to Transmission Electron Microscopy (TEM), which is optimally used for internal structure analysis, SEM visualizes the surface of a material and generates images based on the

reflection of electron beams (Inkson, 2016). SEM focuses an electron beam onto the sample surface, and the interaction of the electrons with the material generates secondary and backscattered electrons to produce high-resolution images. Because of the ability of high-energy electron beams to cause sample charging and potential damage, insulating materials require special preparatory techniques. These can involve the deposition of a conductive coating and examination at lower accelerating voltages (1–4 kV) (Egerton & Egerton, 2016; Goldstein et al., 2003). One of the widely utilized techniques of specimen preparation is the procedure of ion sputter coating with a conductive material, such as gold, platinum, carbon, or palladium, under argon gas because of its high atomic mass, inertness, and non-destruction (Goldstein et al., 2003; Hatano et al., 2022). SEM examination is conducted under a vacuum chamber, where the radiated electron beam (accelerated between 0.1–50 keV voltage) is concentrated and scanned in a sequence over the sample surface. Low vacuum pressure ($0.1-10^{-4}$ Pa) helps in reducing the electron-air interactions, which results in better image quality (Goldstein et al., 2017). SEM imaging can be conducted on the sample surface, while cross-sections can be obtained using fracture or microtomy (Mitchell & Tojeira, 2016).



Figure 3.5. Scanning Electron Microscope.

For the present work, morphologies and microstructures of the samples were examined with the help of field-emission scanning electron microscopy (JEOL-IT500, JEOL Co., Ltd., Tokyo, Japan) at a 10 kV accelerating voltage. Surface specimens were trimmed from the films using stainless steel scissors and mounted on aluminum pin stubs with copper adhesive tape. Also, cross-sectional specimens of each film type were prepared by immersing sections in liquid nitrogen and fracturing them with a razor blade to expose a clean cross section, The specimens were mounted on pin stubs with copper tape and were coated with an approximate 100 Å of platinum by ion sputtering in a sputter-coating machine (EM-ACE600, Leica Co., Ltd., Laughton, England), as presented in Figure 3.5. Sputtering in the argon atmosphere (10–15 psia) was done at a pressure of 50 mTorr and 45 mA current for 45 seconds to achieve uniform conductivity and image contrast. Surface morphology was imaged on 1 specimen each of paper and paper/CNF-5 at 4 levels of magnifications, and on 1 specimen of paper/CNF-5/PGA at 3 levels of magnifications.

Cross-sectional morphology was examined on each film type with 3 levels of magnifications. Images were analyzed in ImageJ to measure total multilayer thickness and individual coating thickness.

3.3.5. Surface Roughness Evaluation

Surface roughness, often called surface morphology in 3D (topography), quantifies the irregularities on a material's surface (Mirabal et al., 2023). This property is crucial in structural integrity and environmental interactions, influencing wettability, wear behavior, and mechanical stresses (Antonov et al., 2023; Song et al., 2022). Surface roughness can be analyzed using 3D microscopic imaging and Z-stack (or focus-stack) techniques, where multiple images taken at different focal distances are combined to create a composite image with an extended depth of field (Johnson, 2008). By filtering the reference plane to align with the actual surface of the film, height variability is minimized, addressing the well-documented limitation of reduced depth of field in high-magnification numerical apertures. Digital microscopes enable surface roughness analysis by capturing topographical features through a high-resolution camera and a wide-range zoom lens, both mounted on a free-angle observation stand. The instrument's Z-axis lens is adjustable, shifting the focus level across the surface. While imaging, the highest points of the sample are recorded first, while the lowest points are recorded last. By tracking the focal plane positions at different heights, the system reconstructs a 3D surface model, facilitating the evaluation of roughness and waviness. This surface micro-geometry is quantitatively described using S_a (arithmetical mean height over an entire surface area) (Woch et al., 2022). S_a provides a comprehensive roughness measurement across the sample's entire surface (Adamčík et al., 2023; Lovely et al.; Lovely et al., 2025). In this study, surface roughness measurements

were performed using a 3D surface profilometer (VK-X3000, Keyence Co., Ltd., Osaka, Japan) depicted in Figure 3.6, adhering to ISO 25178 standards. Three-dimensional surface images of the film samples were analyzed using Keyence VK-X3000 Multifile Analyzer (Keyence Corporation, Osaka, Japan) software, which applied a filtering process to align the reference plane with the film's actual surface, thereby minimizing height variability before roughness parameter quantification. The arithmetical mean height (S_a), representing the average absolute height variation across the defined measurement area, was recorded as the mean of 3 replicates for the Paper and Paper/CNF-5 samples, and 10 replicates for the Paper/CNF-5/PGA sample to ensure statistical reliability.



Figure 3.6. 3D Surface profilometer¹ Instrument.

¹ <https://nanoscience.ucf.edu/equipment/details/surface-profiler-3d-keyence-vk-x3000/>

CHAPTER 4

4. Results and Discussion

4.1. Thermal Stability

Thermogravimetric Analysis (TGA) was used to assess the heat resistance and decomposition behavior of dual-layer biodegradable packaging films. Special focus was given to the effect of a spray-coated PGA layer on a CNF-treated paper substrate. Measurements were conducted under a nitrogen atmosphere. For each of the 4 sample types (Paper, Paper/CNF-5, Paper/CNF-5/PGA, and neat PGA), 3 separate specimens were analyzed and each TGA run was performed 3 times to ensure reproducibility. Figure 4.1 illustrates the TGA curves, with Paper and Paper/CNF-5 showing near-identical profiles, due to the fact that they are both comprised of cellulose. The evaporation of loose and bound water constitutes the first stage of weight loss and occurs in the Paper, Paper/CNF-5, and Paper/CNF-5/PGA samples below approximately 150 °C. This initial weight loss is attributed to the desorption of moisture from hydrophilic and cellulose-based component. Beyond this temperature, the weight of the samples remained largely stable until the onset of major decomposition. The main decomposition stage involves the degradation of the sample's structural framework. According to Table 4.1, the temperature at 5% weight loss ($T_{d5\%}$) occurred at 278 °C for the Paper sample, 277 °C for Paper/CNF-5, and 271 °C for Paper/CNF-5/PGA. These values indicate that all three systems possess appreciable thermal endurance. As shown in Figure 4.1, all samples exhibited nearly identical thermal behavior. The addition of CNF to the paper layer had little impact on the decomposition pattern. The Paper/CNF-5/PGA sample includes an additional biopolymer layer. Despite

this, its Td_{5%} value remained relatively high at 271 °C, slightly lower than Paper and Paper/CNF-5 but slightly higher than neat PGA at 266 °C. This suggests that the presence of the paper and CNF layers slightly improved the early thermal stability of the PGA within the multilayer system. PGA's known characteristics, including high crystallinity (typically 45 to 55%), tightly packed molecular structure, and limited segmental mobility, are responsible for its strong thermal behavior, even when used as a distinct layer over the paper/CNF substrate. Compared to conventional a biodegradable polyester such as PLA, PGA continues to demonstrate superior thermal resistance, making it a reliable candidate for dual-layer bio-based systems (Ayyoob et al., 2017; Murcia Valderrama et al., 2020; Yu et al., 2016). Although triethyl citrate (TEC), with a boiling point of 294 °C, was used in the suspension, the TGA curve exhibited a single, well-defined degradation peak starting at 271 °C, consistent with neat PGA. This indicates that the residual TEC likely volatilized concurrently with the PGA degradation rather than appearing as a separate peak, due to the proximity of TEC's boiling point to PGA's degradation onset temperature.

The residual mass observed at the end of thermal decomposition further highlights the influence of each component in the samples. The Paper/CNF-5 sample yielded the highest residual mass (~15%), which typically occurs due to the presence of minor inorganic impurities or structural modifications introduced during the nanofiber extraction process (Hameed et al., 2022; Roman & Winter, 2004). Such impurities or structural changes commonly enhance char formation, leading to increased residue at elevated temperatures compared to the paper alone (~12%). Introducing the PGA layer to the Paper/CNF-5 substrate resulted in a lower residual mass (~12%), closer to the paper itself. This indicates that PGA contributes minimal residue compared to Paper and CNF-5 upon

decomposition, since if it had higher residue compared to Paper, the residue of Paper/CNF-5/PGA would be much higher than Paper alone. PGA predominantly decomposes into volatile compounds without significant residue formation due to its aliphatic polyester structure (Yang et al., 2021). Additionally, the plasticizer, TEC, volatilizes entirely during heating and leaves no substantial residue (Vieira et al., 2011).

Table 4.1. Thermogravimetric analysis of dual-Layer packaging films: Major degradation temperatures.

Samples	T _{d5%} (°C)	T _f (°C)
Paper	278	366
Paper/CNF-5	277	369
Paper/CNF-5/PGA	271	368
PGA	266	375

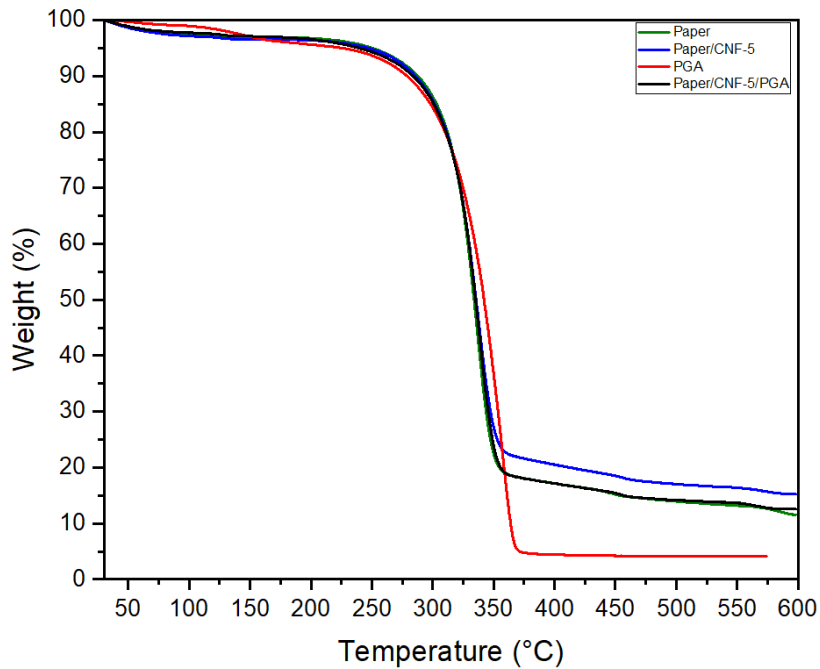


Figure 4.1. Thermogravimetric weight loss profile of dual-layer packaging films under N₂.

4.2. Surface Roughness

Following thermal analysis, surface roughness was measured to assess how each coating step affects the overall and surface-specific layer build-up. A 3D surface profiler provided precise measurements of total and coated layer roughness. Surface roughness

influences the barrier properties of paper-based materials, particularly when modified with biopolymer coatings. In this study, 3D surface profilometry was employed to assess the topographical characteristics of sample types: Paper, Paper/CNF-5, and Paper/CNF-5/PGA. For each sample type, 3 separate specimens of Paper and Paper/CNF-5 and 10 specimens of Paper/CNF-5/PGA were measured to ensure statistical reliability of the S_a values. The arithmetic mean height (S_a) values were measured to quantify surface roughness, providing insights into the effectiveness of each treatment. As shown in Figure 4.2, the Paper sample exhibited a surface roughness with a S_a value of $3.83 \pm 0.45 \mu\text{m}$. Compared to the unpressed paper sample (Table S1), this roughness level reflects the improved yet still relatively rough surface of the hot-pressed mulberry fiber paper, especially when compared to the coated variants. Despite the hot pressing, the fibrous and porous characteristics remain evident, impacting its barrier properties and printability and limiting its applicability in high-quality packaging solutions. Incorporating CNF into the paper matrix (Paper/CNF-5) resulted in a significant reduction in surface roughness, with the S_a value decreasing to $2.15 \pm 0.64 \mu\text{m}$. This improvement is likely due to forming a more uniform and denser network upon hot pressing, which minimizes surface irregularities and leads to a smoother finish. With an average S_a value of almost $1.33 \mu\text{m} \pm 0.05 \mu\text{m}$, the Paper/CNF-5/PGA samples showed the most noticeable improvement in surface smoothness. Applying the PGA layer, followed by hot pressing, likely facilitated the polymer's flow into residual surface voids, creating a continuous and uniform coating. Figure 4.3 provides supporting 3D and z-stack images, visually confirming the progressive surface smoothing across all three samples. This significant decrease in surface roughness, reflected by the trend of S_a values decreasing from Paper to Paper/CNF-5 to Paper/CNF-

5/PGA, demonstrates how successive biopolymer treatments combined with controlled hot pressing effectively improve surface smoothness, consistent with previous findings on the role of biopolymer coatings in enhancing paper substrates (Khwaldia et al., 2010).

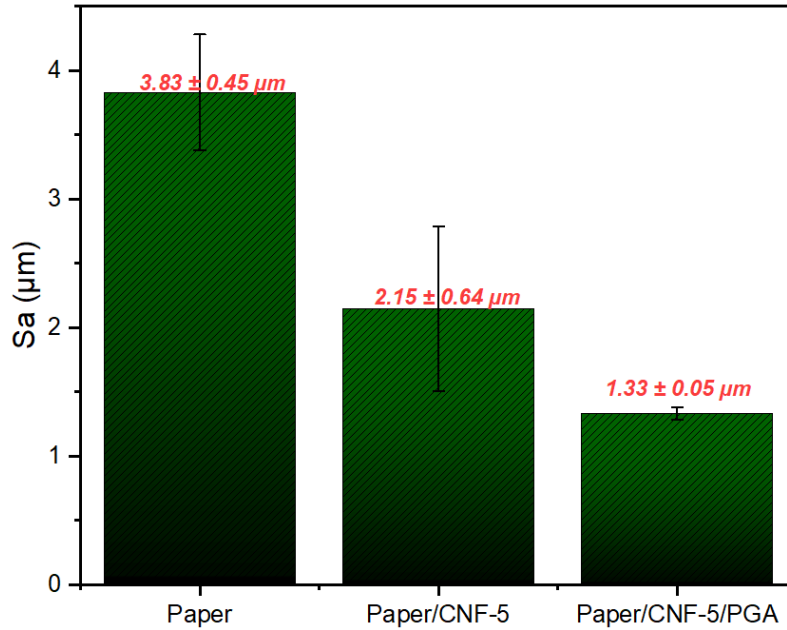
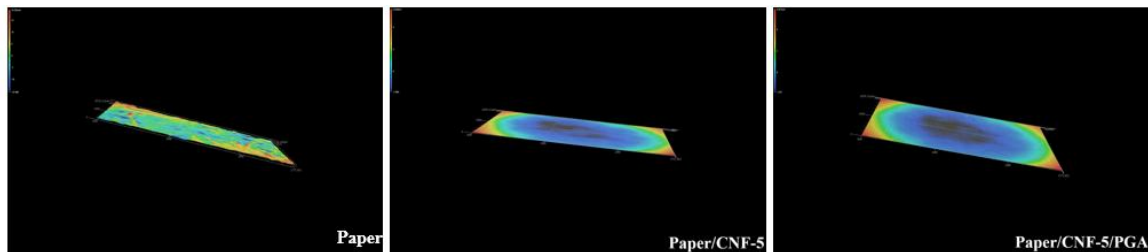
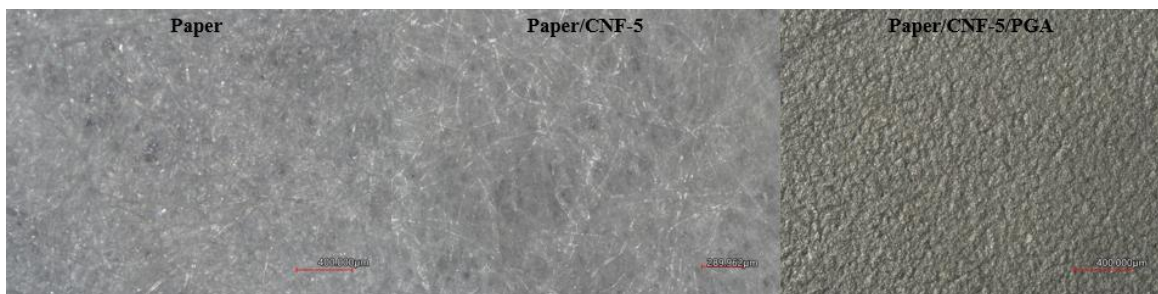


Figure 4.2. Surface roughness of dual-layer packaging films: arithmetical mean height or S_a .



(a)



(b)

Figure 4.3. Surface roughness of dual-layer packaging films (a) 3D and (b) z-stack images.

4.3. Scanning Electron Microscopy (SEM)

SEM was used to examine the morphological structure of the samples on both the surface and cross-section levels. SEM possesses high-resolution imaging to enable close visualization of topography, porosity, and layer interfaces of coated materials. It is beneficial in packaging research to characterize barrier coatings, observe polymer distribution, and evaluate surface smoothness and layer continuity (Ajitha et al., 2016; Yuan et al., 2016). These capabilities are critical for evaluating how spray-coated CNF and PGA alter the microstructure of paper to improve functional properties for packaging applications. SEM analysis was performed on one specimen each of paper, Paper/CNF-5, and Paper/CNF-5/PGA. For surface morphology, 5 images at different magnifications were collected for each of the paper and Paper/CNF-5 specimens, and 6 images for the Paper/CNF-5/PGA specimen. Cross-sectional morphology was examined on each specimen with 3 images per sample. In Figure 4.4, the surface micrograph of Paper shows a rough, porous structure with large voids and gaps between the cellulose fibers, typical of uncoated commercial paper. These surface pores are open and irregular, indicating minimal resistance to moisture or gas penetration. Such morphology is consistent with prior reports describing sack kraft or writing and printing papers, where large fiber-fiber crossings and insufficient bonding between layers result in high porosity and poor barrier properties (de Oliveira et al., 2022; Mirmehdi, de Oliveira, et al., 2018). This open structure is unsuitable for most food or pharmaceutical packaging applications, which need fluid and vapor transmission. In contrast to the uncoated paper, after spray coating the paper with CNF and hot pressing, the surface of Paper/CNF-5 exhibits clear morphological changes. As seen in the SEM surface, the CNF layer covers the substrate uniformly, filling many of the surface

voids and reducing the average pore size. The fibrous texture of the paper is still visible beneath the nanocellulose matrix, but the overall surface is significantly smoother. These changes show that the CNF suspension penetrated the surface and filled voids during spray coating. Hot pressing then consolidated the layer, making it denser. This observation aligns with reports that CNF forms a dense web over porous paper, reducing porosity and improving barrier function by forming a tortuous path against molecular diffusion (Mirmehdi, de Oliveira, et al., 2018; Wang et al., 2018). The smoother surface obtained after CNF spray over paper coating is also associated with increased contact angle and hydrophobicity, as documented (Torun & Onses, 2017). Upon adding a second spray-coated layer of PGA to the Paper/CNF-5 sample, the SEM surface image of Paper/CNF-5/PGA reveals a further transformation. As observed in Figure 4.4, the outer surface appears continuous and highly smooth, with minimal evidence of underlying fiber texture. Compared to Paper/CNF-5, the topography of this sample is more uniform, and most surface roughness is eliminated. This smoothing is attributed to the second spray-coated layer of PGA, which spreads over the CNF-treated substrate and fills any remaining gaps. During hot pressing, the PGA softens and conforms tightly to the CNF layer and underlying paper, forming a dense surface layer. However, PGA films commonly exhibit cracking phenomena, such as microcracks and pinholes, particularly after thermal processing or solvent casting, primarily due to their inherent brittleness and high crystallinity, especially in the absence of a plasticizer (Shum & Mak, 2003). In Figure 4.4, the SEM images of the Paper/CNF-5/PGA sample reveal a continuous and uniform outer surface with only a few observable cracks. This smooth morphology is a result of the cohesive polymer coverage achieved during hot pressing. The limited occurrence of surface cracks might be attributed

to the incorporation of 10 wt.% TEC as the plasticizer, which enhances polymer chain mobility and flexibility. By softening the otherwise brittle PGA matrix, TEC enables better surface flow and film formation, resulting in a denser, more cohesive layer that minimizes potential diffusion pathways and reduces the likelihood of pinhole formation. The impact of TEC on the PGA surface morphology is highlighted by comparing samples with and without plasticizers (Figure S2).

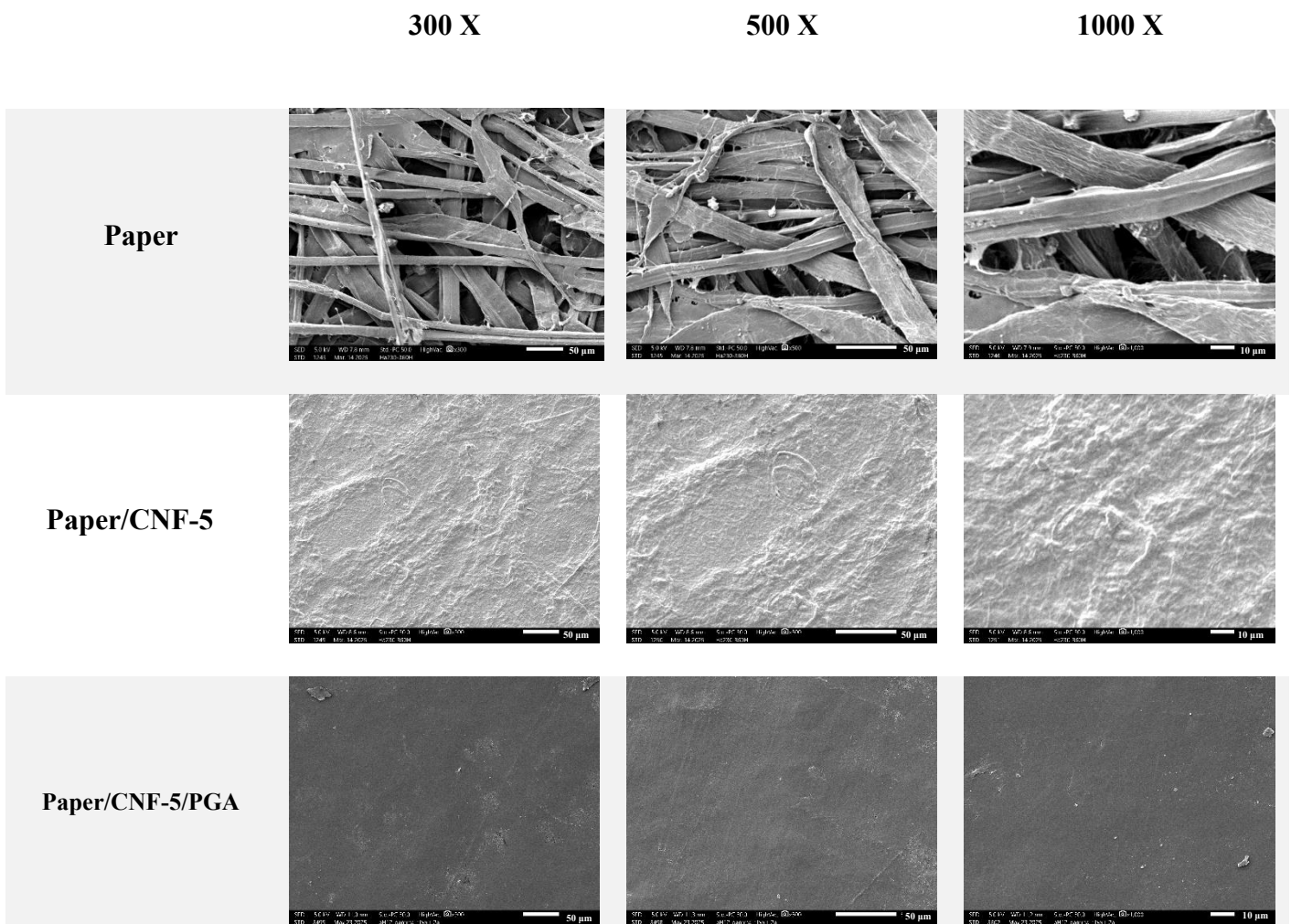


Figure 4.4. SEM surface images of dual-layer packaging samples.

To gain a deeper understanding of these structural characteristics, cross-sectional SEM analysis was conducted on the samples. Thickness values reported in this section are

based on a single representative measurement for each sample, intended for comparative evaluation of layer dimensions rather than statistical analysis. In the Paper sample, the coated layer thickness was measured at approximately 103.7 micrometers, with no visible coating layer on the surface (Figure 4.5; Table 4.2). Although the substrate was hot pressed, the internal structure remains composed of loosely packed cellulose fibers. The absence of a coating layer allows the persistence of surface pores and inter-fiber voids, as also observed in the surface SEM images, which contributes to the lack of barrier functionality in this unmodified paper sample. In the case of Paper/CNF-5, the coated layer thickness was measured at 97.2 micrometers, and the top surface exhibited a noticeable coated layer of about 6.2 micrometers, as shown in Figure 4.5 and Table 4.2. This coated layer represents the deposited CNF, which is compacted through hot pressing. Although thin, the layer exhibits good adhesion to the paper and reduces surface porosity, as evidenced by the dense microstructure in the cross-section. Finally, for the Paper/CNF-5/PGA sample, the cross-sectional image of Paper/CNF-5/PGA reveals the most substantial coating among the three samples. The thickness of the sample is measured at 61.8 micrometers, and the top-coated layer is approximately 20.9 micrometers (Table 4.2). Due to the similar morphology and elemental composition of CNF and PGA, their individual layers could not be distinguished in the cross-sectional SEM images. This thickness reflects the combined contribution of the CNF and PGA layers, with PGA comprising the majority. The interface between the coated layer and the paper is continuous, with no observable delamination or gaps. This indicates strong interfacial adhesion, likely governed by mechanical interlocking and physical bonding between the polymer and the microstructured CNF surface beneath. The notable increase in top layer thickness

correlates with improved barrier functionality, as thicker, denser surface layers reduce the permeation of gases and oils (Wang et al., 2018; Yuan et al., 2016). The SEM images demonstrate that the prepared PGA suspension was effective for spray coating, as confirmed by surface and cross-sectional images showing uniform coating coverage and good interlayer adhesion, fulfilling the first objective of forming a stable dual-layer structure. To further assess the role of the plasticizer, SEM images of PGA coated samples prepared without TEC (Figures S2 and S3) indicate that while these samples exhibited acceptable interlayer adhesion, confirming the suitability of the PGA suspension for spray coating, surface images revealed significant cracks and defects.

Table 4.2. Cross-sectional thickness measurements of the whole and coated layers for each sample, obtained from SEM analysis.

Sample	Thickness of the Whole Layer	Thickness of the Coated Layer
Paper	103.703 μm	N/A
Paper/CNF-5	97.157 μm	6.181 μm
Paper/CNF-5/PGA	61.760 μm	20.851 μm

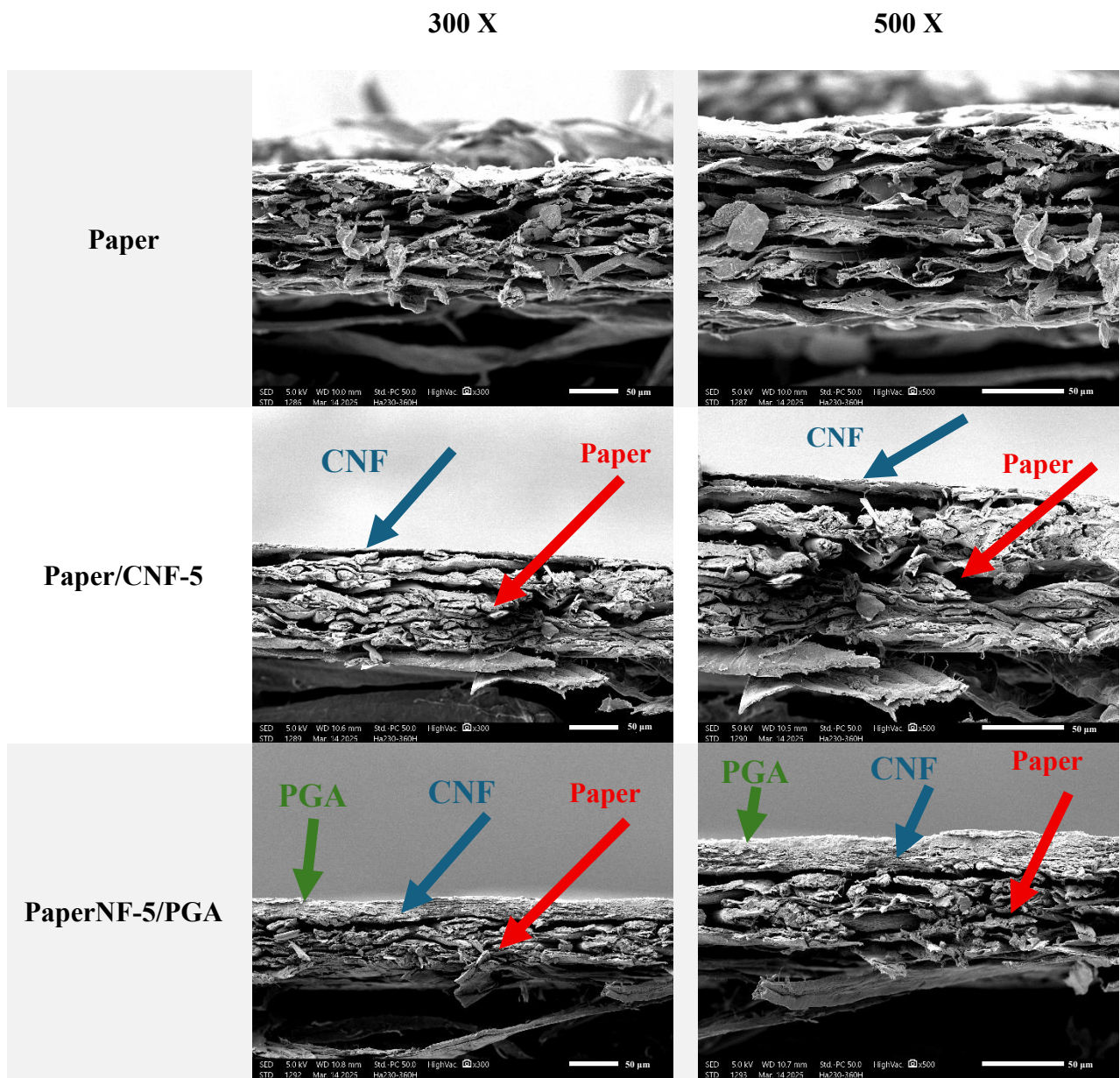


Figure 4.5. SEM cross-sectional images showing the dual-layer packaging systems.

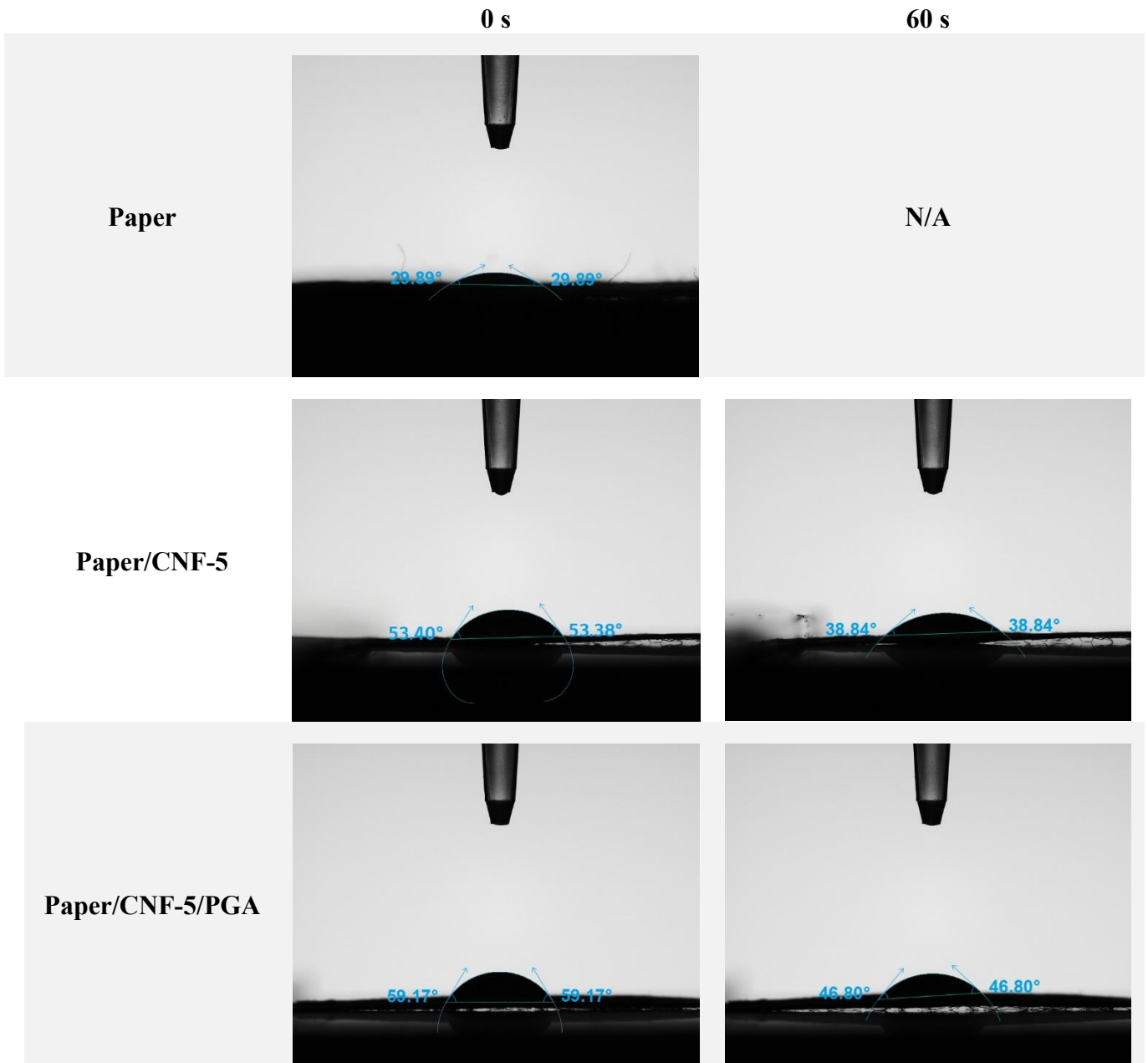
4.4. Wettability or Contact Angle

Contact angle measurements were performed to evaluate changes in surface functionality. Hydrophobicity reflects surface energy and barrier efficacy against moisture.

Contact angles of selected samples were measured in order to investigate these concepts. These results highlight the impact of surface treatments on water resistance. To establish a baseline, the study first examined a neat paper sample. The commercial paper sample displayed extreme hydrophilicity. Upon depositing a water drop, the droplet immediately began to penetrate and spread into the porous fibrous network. The bare paper absorbed water almost instantly, with the droplet vanishing within 1 second ($\theta \approx 0^\circ$). This is typical for cellulose substrates with hydroxyl-rich, porous structures that promote capillary absorption (Ambrosia & Ha, 2018; Negro et al., 2023). Coating the paper with CNF and applying hot pressing reduced surface roughness, altering its wetting behavior. The initial contact angle of the Paper/CNF-5 sample increased to around 50° , and the water droplet remained visible throughout the 60-second measurement, though it gradually flattened. Although CNF is hydrophilic, its dense fibrillar structure delayed water uptake and stabilized the droplet shape (Lovely et al., 2025; Marchetti et al., 2024; Negro et al., 2023). To build on the CNF coating's moderate success, a layer of PGA was added to enhance water resistance further. Further enhancement in hydrophobicity was observed in the Paper/CNF-5/PGA sample. This sample exhibited the highest initial and sustained contact angles among the three, with the droplet maintaining a slightly more spherical shape even at 60 seconds. The surface roughness further declined upon PGA coating, indicating a smoother and more continuous surface layer. PGA contributes to this hydrophobic behavior through its inherent chemical structure, a linear aliphatic polyester lacking free hydroxyl groups, making it inherently less polar and less hydrophilic than cellulose. PGA is not highly water-repellent; a smooth PGA film has a contact angle of approximately 50 – 55° , which is still considered hydrophilic (Vargha-Butler et al., 2001). However, it attracts

water less than sugar-based CNF. Additionally, PGA's high crystallinity limits the space and movement within the material, making it harder for water to diffuse into or swell the PGA layer. While PGA's surface energy doesn't make it highly water-repellent, its physical structure still prevents water from soaking in quickly. In effect, the droplet remains on the surface as an isolated bead for longer (Ambrosia & Ha, 2018; Regubalan et al., 2022). The improvements in water resistance from CNF and PGA coatings can be attributed not only to changes in surface chemistry but also to the effect of hot pressing. This process has likely enhanced film uniformity, polymer diffusion, and coating adhesion. Hot pressing also promotes densification, minimizing surface irregularities and sealing microscopic voids that might otherwise act as wicking pathways. These combined effects are supported by the observed gradation in surface roughness and by the fact that hot-pressed films consistently exhibited higher and more stable contact angles over time, as seen in Figure 4.6.

(a)



(b)

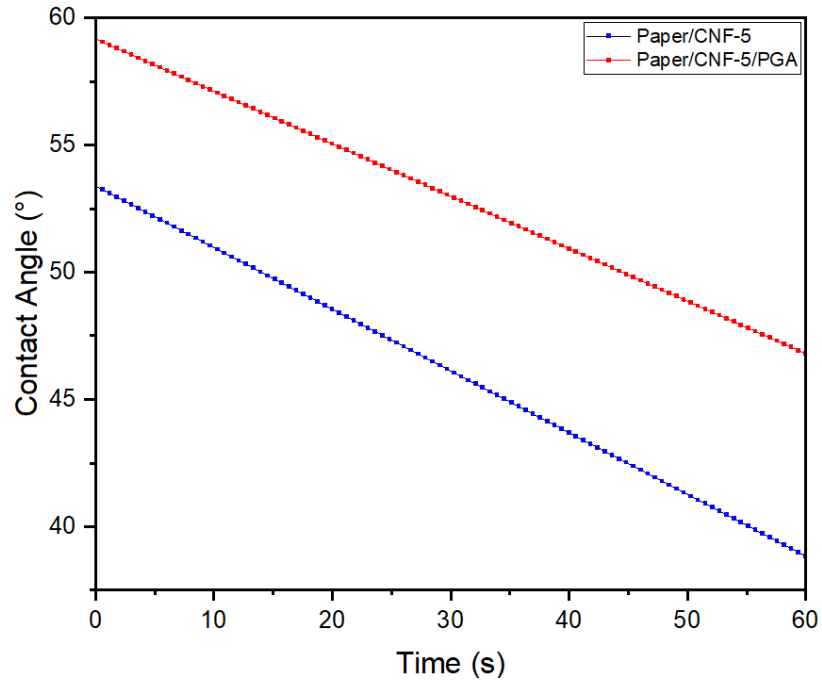


Figure 4.6. Contact angle measurements of dual-layer packaging films: (a) top surface at 0 and 60 seconds, and (b) top surface over 60 seconds.

4.5. Barrier Properties

Barrier properties, particularly oxygen transmission rate (OTR), are critical for evaluating packaging materials intended to protect sensitive products from environmental deterioration (Siracusa, 2012). OTR of uncoated paper was not measured due to its inherently porous structure, which results in very high permeability to gases, rendering accurate measurement impractical or meaningless. As a result, OTR measurements were performed on two sample types, Paper/CNF-5 and Paper/CNF-5/PGA, using one specimen of each tested in three replicate cycles. The averaged values in Table 4.3 and Figure 4.7 demonstrate the significant barrier enhancement provided first by CNF deposition and then by the addition of the PGA layer. The OTR of the uncoated paper sample was beyond the detection limit due to its inherently porous structure characterized by loosely packed fibers.

This open fiber network allows unobstructed oxygen diffusion, confirmed by SEM analyses, which displayed numerous fiber voids facilitating oxygen permeability (Ayranci & Tunc, 2003; Mirmehdi, Hein, et al., 2018). It is noteworthy that samples coated with PGA without plasticizer showed no barrier properties, which may be attributed to the presence of surface cracks and defects observed in SEM images (Figure S2). Applying CNF (Paper/CNF-5) reduced the OTR significantly to 27.00 ± 0.87 cc/(m²·24h), whereas uncoated paper is so highly porous that its OTR is beyond the instrument's measurable range. This shows CNF's effectiveness as a barrier by physically blocking oxygen diffusion. SEM images show a more compact surface with filled inter-fiber voids, creating difficult paths that slow oxygen movement. Profilometry data also confirms reduced surface roughness after CNF application, suggesting fewer surface irregularities that could allow oxygen to pass (Hong & Krochta, 2006; Miller & Krochta, 1997; Mirmehdi, Hein, et al., 2018; Shanmugam, 2022). Adding the PGA layer (Paper/CNF-5/PGA) further reduced OTR to 1.63 ± 0.37 cc/(m²·24h), indicating a strong barrier performance approaching high-barrier standards. The superior barrier property of PGA is primarily due to its high crystallinity and dense molecular packing, creating a tortuous pathway that effectively restricts oxygen permeation. SEM micrographs reveal a continuous and dense PGA layer effectively sealing remaining surface openings left after CNF application. This improvement corresponds with decreased surface wettability; higher contact angles suggest lower surface energy and better impermeability (Regubalan et al., 2022; Samantaray et al., 2020).

Table 4.3. Oxygen transmission rate values of dual-layer packaging samples.

Sample	Composition Thickness (μm)	Oxygen Transmission Rate ($\text{cc}/(\text{m}^2 \cdot 24\text{h})$)	Oxygen Transmission Rate Coefficient ($\text{cc} \cdot \text{cm}/(\text{cm}^2 \cdot \text{s} \cdot \text{cmHg}) \times 10^{-13}$)
Paper/CNF-5	81.00 ± 0.89	27.00 ± 0.87	33.30 ± 1.07
Paper/CNF-5/PGA	104.00 ± 1.73	1.63 ± 0.37	1.62 ± 0.62

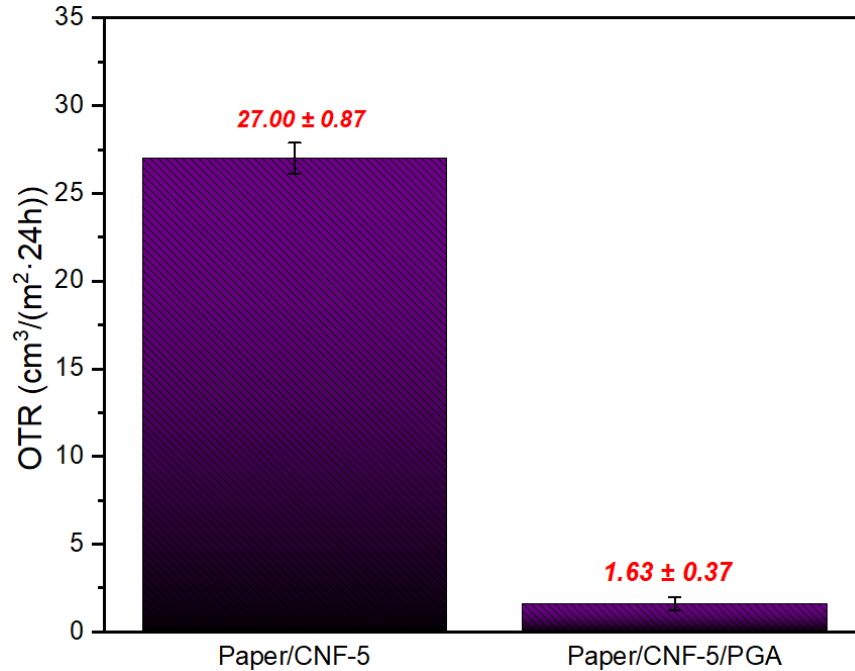


Figure 4.7. Oxygen transmission rate of Paper, Paper/CNF-5, and Paper/CNF-5/PGA samples.

When comparing this performance with benchmark materials shown in Table 4.4 (Regubalan et al., 2022), the Paper/CNF-5/PGA dual-layer demonstrates superior barrier properties compared to most biopolymers listed. It notably outperforms biopolymers such as PLA and approaches the effectiveness of well-known high-barrier synthetic polymers. However, the OTR is slightly higher compared to the neat PGA referenced in Table 4.4. This difference is likely due to residual surface pores and minor microcracks generated during spray coating and hot pressing processes. Additionally, the neat PGA from Table 4.4 originates from another source with potentially different properties, further contributing to this observed discrepancy. Spray coating CNF and PGA on paper thus effectively

enhance oxygen barrier performance, establishing this dual-layer system as a promising sustainable packaging solution.

Table 4.4. Comparison of the oxygen transmission rate of the dual-layer sample with various polymers.

Material	Oxygen Permeability¹
PGA	0.036
Paper/CNF-5/PGA	0.27±0.10
PLA	38-42
HDPE	130-185
PP	150-800
PA	2-3
PET	3-6
PVC	4-30
EVOH	2-2.6

¹ cm³·mil/(100 in²·day·atm)

5. Conclusion

The study demonstrates that a dual-layered system of a hot-pressed paper substrate impregnated with CNF and a spray-coated PGA outer film achieves thermal and barrier properties comparable to or exceeding many conventional bioplastics. Using a solvent-exchange approach that replaced hexafluoroisopropanol (HFIP) and dichloromethane (DCM) with ethanol, successive spray coating and hot pressing produced a smooth PGA film with minimal surface cracking PGA film on a dense CNF-reinforced paper substrate. The thermogravimetric analysis demonstrated pyrolytic stability up to 270 °C, indicating suitability for biodegradable packaging applications demanding mechanical integrity at elevated temperatures (Diana et al., 2022). Surface profilometry indicated progressive smoothing, and SEM micrographs revealed a homogeneous PGA layer supported by CNF that had infiltrated the native pores of the paper. Enhanced smoothness presumably reduces diffusion pathways for moisture and gases, correlating with observed oxygen transmission rate reductions, thereby enhancing packaging performance. The superior surface finish makes the Paper/CNF-5/PGA system suitable for food packaging, where aesthetic and barrier properties are crucial (Moghimi et al., 2018). SEM analysis confirmed that CNF reduced porosity and PGA formed a continuous barrier layer, enhancing structure and function. Water contact angle tests showed hydrophobic enhancement, with angles around 60°, remaining above 45° after 60 seconds. This dual-layer approach controls wettability and possibly prolongs shelf life and performance integrity for moisture-sensitive packaging applications. Oxygen transmission rates notably decreased to $1.6 \text{ cm}^3 \cdot \text{m}^{-2} \cdot 24 \text{ h}^{-1}$ with the PGA coating, attributable to PGA's crystalline structure and tortuous diffusion pathways, significantly outperforming cellulose-based layers alone.

5.1. Summary of Objectives and Outcomes

- **Objective 1:** Formulate a stable PGA–ethanol suspension for spray coating
 - *Achieved.* A homogenous, sprayable suspension was prepared via HFIP/DCM replacement.
- **Objective 2:** Construct a PGA–paper dual-layer system with CNF as pore-filling bridge
 - *Achieved.* SEM confirmed CNF infiltration and continuous PGA coverage.
- **Objective 3:** Optimize hot-press parameters (temperature, pressure, dwell time) with fixed CNF/PGA loadings
 - *Partially achieved.* While the hot-pressing conditions were set at 130 °C for 15 minutes under 4.14 MPa for CNF-coated paper and at 225 °C for 2 minutes under 8.27 MPa for the PGA-coated samples, it should be noted that these values represent the set points on the hot-press instrument. The actual temperatures between the stainless-steel mirror plates were not directly measured and may have varied. This introduces a degree of uncertainty, especially for the PGA layer, which is highly sensitive to thermal conditions due to its narrow processing window. Despite this, both layers were successfully hot-pressed and formed uniform coatings with good adhesion based on SEM imaging, though future studies should include direct temperature monitoring to confirm precise processing conditions.
- **Objective 4:** Characterize films by TGA, SEM, OTR, contact angle, and surface roughness

- *Achieved.* All analyses confirmed enhanced thermal stability, barrier performance, hydrophobicity, and smoothness.

5.2. Limitations

The limited data set collected here should be replicated for greater certainty and to identify future improvements. The high cost of PGA and its conventional solvents notably increases material expenses, posing a challenge for large-scale applications. Even after diluting and substituting with ethanol, safety concerns and handling requirements related to fluorinated and chlorinated solvents add operational complexity. Additionally, the experimental procedures involved in preparing and coating PGA suspensions are highly complex and labor-intensive, making them susceptible to human error. The complexity of this methodology demands careful optimization to enhance reproducibility and reduce processing inaccuracies. The highly porous and structurally heterogeneous nature of the mulberry fiber-based paper used in this study also posed challenges during spray coating, including material penetration, hole formation, and inconsistent surface coverage. Another critical limitation arises from the inherently narrow processing window of PGA, specifically due to its proximity between melting and thermal decomposition temperatures. Precise temperature control during hot pressing is thus essential, as deviations can result in defects such as incomplete melting or thermal degradation of the PGA layer. Furthermore, due to the similar morphology and overlapping appearance of CNF and PGA in cross-sectional SEM images, it was not possible to distinguish their individual layers or quantify their respective contributions to the total coated thickness. Complementary techniques such as Fourier Transform Infrared Spectroscopy (FTIR) mapping or Raman imaging would be required to distinguish between the CNF and PGA in future studies. Scaling the spray

coating and hot pressing processes beyond laboratory-scale will also require additional engineering solutions to maintain consistent material usage, layer uniformity, and temperature control across larger surface areas. Finally, the validation of the developed dual-layer packaging system would benefit from increased sample replication and additional characterization tests, such as water vapor transmission rate (WVTR) analysis and mechanical properties like tensile strength, to thoroughly confirm the material's suitability for practical packaging applications.

5.3. Recommendations for future research

- Selecting more structurally uniform and mechanically robust paper substrates with lower porosity and smoother surfaces to improve coating performance and reduce the need for excessive filler materials. Lab-fabricated papers with controlled thickness and fiber distribution may prevent spray-induced damage and minimize penetration of large-particle suspensions, enabling more consistent barrier layer formation
- Exploring customized or synthesized PGA variants with tailored molecular weight, co-monomer incorporation, or surface functionalization to improve processability and broaden the thermal processing window. While such modifications may slightly compromise barrier and thermal performance, they can be suitable for packaging systems with moderate requirements and may simplify processing

- Optimizing solvent systems to produce a stable, fine-particle PGA suspension suitable for spray coating while minimizing or eliminating the use of hazardous fluorinated and chlorinated solvents
- Investigating waterborne formulations or alternative green solvents for PGA to improve safety and reduce processing complexity
- Developing a solvent recovery and recycling system for HFIP and DCM to reduce environmental impact and material cost
- Exploring alternative biopolymer substrates for the base or intermediate layer to improve interfacial adhesion, processability, and property customization
- Improving process control for hot pressing by developing temperature-feedback systems or adaptive heating platforms to accommodate PGA's narrow processing window and reduce thermal damage
- Expanding the experimental dataset through larger-scale replication and statistical analysis to improve confidence in the reproducibility of the oxygen transmission rate of PGA dual-layer packaging
- Conducting additional mechanical and moisture barrier properties analysis, including water vapor transmission rate (WVTR) and tensile strength, to evaluate the dual-layer system's packaging performance comprehensively

References

- Adamčík, L., Dzurenda, L., Banski, A., & Kminiak, R. (2023). Comparison of surface roughness of beech wood after sanding with an eccentric and belt sander. *Forests*, *15*(1), 45.
- Ajitha, A., Aswathi, M., Maria, H. J., Izdebska, J., & Thomas, S. (2016). Multilayer polymer films. *Multicomponent polymeric materials*, 229-258.
- Alias, A., Wan, M. K., & Sarbon, N. (2022). Emerging materials and technologies of multi-layer film for food packaging application: A review. *Food Control*, *136*, 108875.
- Ambrosia, M. S., & Ha, M. Y. (2018). A molecular dynamics study of Wenzel state water droplets on anisotropic surfaces. *Computers & Fluids*, *163*, 1-6.
- Antonov, D. V., Islamova, A. G., & Strizhak, P. A. (2023). Hydrophilic and hydrophobic surfaces: Features of interaction with liquid drops. *Materials*, *16*(17), 5932.
- Anukiruthika, T., Sethupathy, P., Wilson, A., Kashampur, K., Moses, J. A., & Anandharamakrishnan, C. (2020). Multilayer packaging: Advances in preparation techniques and emerging food applications. *Comprehensive Reviews in Food Science and Food Safety*, *19*(3), 1156-1186.
- Araki, T., Shibayama, M., & Tran-Cong, Q. (1998). *Structure and properties of multiphase polymeric materials* (Vol. 46). CRC Press.
- Atiqah, M. N., Gopakumar, D. A., FAT, O., Pottathara, Y. B., Rizal, S., Aprilia, N. S., Hermawan, D., Paridah, M., Thomas, S., & HPS, A. K. (2019). Extraction of cellulose nanofibers via eco-friendly supercritical carbon dioxide treatment followed by mild acid hydrolysis and the fabrication of cellulose nanopapers. *Polymers*, *11*(11), 1813.
- Aulin, C., Gällstedt, M., & Lindström, T. (2010). Oxygen and oil barrier properties of microfibrillated cellulose films and coatings. *Cellulose*, *17*, 559-574.
- Ayranci, E., & Tunc, S. (2003). A method for the measurement of the oxygen permeability and the development of edible films to reduce the rate of oxidative reactions in fresh foods. *Food chemistry*, *80*(3), 423-431.
- Ayyoob, M., Lee, D. H., Kim, J. H., Nam, S. W., & Kim, Y. J. (2017). Synthesis of poly (glycolic acids) via solution polycondensation and investigation of their thermal degradation behaviors. *Fibers and Polymers*, *18*, 407-415.
- Beswick, R., & Dunn, D. (2002). *Plastics in Packaging: Western Europe and North America*. iSmithers Rapra Publishing.
- Borrega, M., & Orelma, H. (2019). Cellulose Nanofibril (CNF) Films and xylan from hot water extracted birch kraft pulps. *Applied Sciences*, *9*(16), 3436.
- Borrelle, S. B., Ringma, J., Law, K. L., Monnahan, C. C., Lebreton, L., McGivern, A., Murphy, E., Jambeck, J., Leonard, G. H., & Hilleary, M. A. (2020). Predicted growth in plastic waste exceeds efforts to mitigate plastic pollution. *Science*, *369*(6510), 1515-1518.
- Boufi, S., González, I., Delgado-Aguilar, M., Tarrès, Q., Pèlach, M. À., & Mutjé, P. (2016). Nanofibrillated cellulose as an additive in papermaking process: A review. *Carbohydrate polymers*, *154*, 151-166.
- Brown, N. (1992). *Plastics in food packaging: properties: design and fabrication* (Vol. 5). CRC Press.

- Brunšek, R., Kopitar, D., Schwarz, I., & Marasović, P. (2023). Biodegradation properties of cellulose fibers and PLA biopolymer. *Polymers*, *15*(17), 3532.
- Budak, K., Sogut, O., & Aydemir Sezer, U. (2020). A review on synthesis and biomedical applications of polyglycolic acid. *Journal of polymer research*, *27*, 1-19.
- Cheng, Q., & Via, B. (2017). Characterization of cellulose fibril aggregates isolated by the combination of ultrasonication and homogenizer. *Wood Material Science & Engineering*, *12*(4), 197-202.
- Cho, S.-W., Gällstedt, M., & Hedenqvist, M. S. (2010). Properties of wheat gluten/poly (lactic acid) laminates. *Journal of agricultural and food chemistry*, *58*(12), 7344-7350.
- Chun, S.-J., Lee, S.-Y., Doh, G.-H., Lee, S., & Kim, J. H. (2011). Preparation of ultrastrength nanopapers using cellulose nanofibrils. *Journal of Industrial and Engineering Chemistry*, *17*(3), 521-526.
- Cobb, S. J., Ayres, Z. J., & Macpherson, J. V. (2018). Boron doped diamond: a designer electrode material for the twenty-first century. *Annual review of analytical chemistry*, *11*(1), 463-484.
- Colomer, I., Chamberlain, A. E., Haughey, M. B., & Donohoe, T. J. (2017). Hexafluoroisopropanol as a highly versatile solvent. *Nature Reviews Chemistry*, *1*(11), 0088.
- Cui, H., Zhang, Z., & Huang, Q. (2025). Enhancing Degradation Resistance of Polyglycolic Acid through Stereocomplex Polylactic Acid Integration: A Novel “Stereo-Lock” Approach. *Polymer*, 128088.
- de Oliveira, M. L. C., Mirmehdi, S., Scatolino, M. V., Júnior, M. G., Sanadi, A. R., Damasio, R. A. P., & Tonoli, G. H. D. (2022). Effect of overlapping cellulose nanofibrils and nanoclay layers on mechanical and barrier properties of spray-coated papers. *Cellulose*, 1-17.
- De Smet, M. (2016). The New Plastics Economy—Rethinking the future of plastics. European Conference on Plastics in Freshwater Environments 21–22 June 2016 in Berlin,
- Del Rio, O., & Neumann, A. (1997). Axisymmetric drop shape analysis: computational methods for the measurement of interfacial properties from the shape and dimensions of pendant and sessile drops. *Journal of colloid and interface science*, *196*(2), 136-147.
- Diana, Z., Reilly, K., Karasik, R., Vegh, T., Wang, Y., Wong, Z., Dunn, L., Blasiak, R., Dunphy-Daly, M. M., & Rittschof, D. (2022). Voluntary commitments made by the world’s largest companies focus on recycling and packaging over other actions to address the plastics crisis. *One Earth*, *5*(11), 1286-1306.
- Du, P., Meng, X., Gong, W., Li, C., Jiang, W., Xu, Y., Jiao, L., & Xin, Z. (2025). Poly (glycolic acid) with Enhanced Mechanical and Foaming Properties Obtained by Biobased Cashew Phenol Glycerol Ether. *Industrial & Engineering Chemistry Research*.
- Egerton, R., & Egerton, R. (2016). The scanning electron microscope. *Physical principles of electron microscopy: An introduction to TEM, SEM, and AEM*, 121-147.
- Ehrmann, K. (2024). Soft Lens Measurement. In *Contact Lens Practice* (pp. 76-89. e72). Elsevier.

- Eslami, H., & Mekonnen, T. H. (2023). Flexible and green multilayer paper coating for barrier enhancement of paper packaging. *Sustainable Materials and Technologies*, 37, e00694.
- Fernández-Santos, J., Valls, C., Cusola, O., & Roncero, M. B. (2021). Improving filmogenic and barrier properties of nanocellulose films by addition of biodegradable plasticizers. *ACS Sustainable Chemistry & Engineering*, 9(29), 9647-9660.
- Fernández-Santos, J., Valls, C., Cusola, O., & Roncero, M. B. (2022). Composites of cellulose nanocrystals in combination with either cellulose nanofibril or carboxymethylcellulose as functional packaging films. *International journal of biological macromolecules*, 211, 218-229.
- Fernandez, M. O., & Trasande, L. (2024). The Global Plastics Treaty: An Endocrinologist's Assessment. *Journal of the Endocrine Society*, 8(1), bvad141.
- Fourati, Y., Magnin, A., Putaux, J.-L., & Boufi, S. (2020). One-step processing of plasticized starch/cellulose nanofibrils nanocomposites via twin-screw extrusion of starch and cellulose fibers. *Carbohydrate polymers*, 229, 115554.
- Fu, Y., & Dudley, E. G. (2021). Antimicrobial-coated films as food packaging: A review. *Comprehensive Reviews in Food Science and Food Safety*, 20(4), 3404-3437.
- Gentile, P., Chiono, V., Carmagnola, I., & Hatton, P. V. (2014). An overview of poly (lactic-co-glycolic) acid (PLGA)-based biomaterials for bone tissue engineering. *International journal of molecular sciences*, 15(3), 3640-3659.
- Goldstein, J. I., Newbury, D. E., Echlin, P., Joy, D. C., Lyman, C. E., Lifshin, E., Sawyer, L., Michael, J. R., Goldstein, J. I., & Newbury, D. E. (2003). Specimen preparation of polymer materials. *Scanning Electron Microscopy and X-ray Microanalysis: Third Edition*, 565-590.
- Goldstein, J. I., Newbury, D. E., Michael, J. R., Ritchie, N. W., Scott, J. H. J., & Joy, D. C. (2017). *Scanning electron microscopy and X-ray microanalysis*. Springer.
- Good, R. J. (1992). Contact angle, wetting, and adhesion: a critical review. *Journal of adhesion science and technology*, 6(12), 1269-1302.
- Granda, L. A., Oliver-Ortega, H., Fabra, M. J., Tarrés, Q., Pèlach, M. À., Lagarón, J. M., & Méndez, J. A. (2020). Improved process to obtain nanofibrillated cellulose (CNF) reinforced starch films with upgraded mechanical properties and barrier character. *Polymers*, 12(5), 1071.
- Gupta, V., Biswas, D., & Roy, S. (2022). A comprehensive review of biodegradable polymer-based films and coatings and their food packaging applications. *Materials*, 15(17), 5899.
- Hameed, S., Wagh, A. S., Sharma, A., Pareek, V., Yu, Y., & Joshi, J. B. (2022). Kinetic modelling of pyrolysis of cellulose using CPD model: effect of salt. *Journal of Thermal Analysis and Calorimetry*, 147(17), 9763-9777.
- Hasselbalch, J. (2025). Toxic growth in the circular economy: is the EU Plastics Strategy a bad policy? *Ineffective Policies: Causes and Consequences of Bad Policy Choices*, 115-129.
- Hatano, T., Nakaba, S., Horikawa, Y., & Funada, R. (2022). A combination of scanning electron microscopy and broad argon ion beam milling provides intact structure of secondary tissues in woody plants. *Scientific Reports*, 12(1), 9152.

- Hernández-García, E., Freitas, P. A., Zomeño, P., González-Martínez, C., & Torres-Giner, S. (2022). Multilayer sheets based on double coatings of poly (3-hydroxybutyrate-co-3-hydroxyvalerate) on paper substrate for sustainable food packaging applications. *Applied Sciences*, *13*(1), 179.
- Hong, S.-I., & Krochta, J. M. (2006). Oxygen barrier performance of whey-protein-coated plastic films as affected by temperature, relative humidity, base film and protein type. *Journal of food engineering*, *77*(3), 739-745.
- Inkson, B. J. (2016). Scanning electron microscopy (SEM) and transmission electron microscopy (TEM) for materials characterization. In *Materials characterization using nondestructive evaluation (NDE) methods* (pp. 17-43). Elsevier.
- Jahangiri, F., Mohanty, A. K., & Misra, M. (2024). Sustainable biodegradable coatings for food packaging: Challenges and opportunities. *Green Chemistry*.
- Johnson, D. (2008). *How to do everything: digital camera*. McGraw-Hill, Inc.
- Johnson, L. M., Mecham, J. B., Krovi, S. A., Caffaro, M. M. M., Aravamudhan, S., Kovach, A. L., Fennell, T. R., & Mortensen, N. P. (2021). Fabrication of polyethylene terephthalate (PET) nanoparticles with fluorescent tracers for studies in mammalian cells. *Nanoscale Advances*, *3*(2), 339-346.
- Khalifeh, S. (2020). 1—Introduction to polymers for electronic engineers. *Polymers in Organic Electronics*, 1-31.
- Khan, M. Q., Kharaghani, D., Nishat, N., Shahzad, A., Hussain, T., Khatri, Z., Zhu, C., & Kim, I. S. (2019). Preparation and characterizations of multifunctional PVA/ZnO nanofibers composite membranes for surgical gown application. *Journal of Materials Research and Technology*, *8*(1), 1328-1334.
- Khwalidia, K., Arab-Tehrany, E., & Desobry, S. (2010). Biopolymer coatings on paper packaging materials. *Comprehensive Reviews in Food Science and Food Safety*, *9*(1), 82-91.
- Kunam, P. K., Ramakanth, D., Akhila, K., & Gaikwad, K. K. (2024). Bio-based materials for barrier coatings on paper packaging. *Biomass Conversion and Biorefinery*, *14*(12), 12637-12652.
- Lettieri, R., Mudassir, M., Domenici, F., Salina, A., Venanzi, M., D'Ottavi, C., Di Bartolomeo, E., & Gatto, E. (2025). Control of Nanoparticle Size of Intrinsically Fluorescent PET (Polyethylene Terephthalate) Particles Produced Through Nanoprecipitation. *Molecules*, *30*(2), 282.
- Li, V. C., Mulyadi, A., Dunn, C. K., Deng, Y., & Qi, H. J. (2018). Direct ink write 3D printed cellulose nanofiber aerogel structures with highly deformable, shape recoverable, and functionalizable properties. *ACS Sustainable Chemistry & Engineering*, *6*(2), 2011-2022.
- Liu, B., Wang, S., Guo, H., Yin, H., Song, Y., Gong, M., Zhang, L., Lin, X., & Wang, D. (2025). High-Strength and Rapidly Degradable Nanocomposite Yarns from Recycled Waste Poly (glycolic acid)(PGA). *Polymers*, *17*(1), 100.
- Liu, C., Yan, G., Gao, J., Guo, H., & Hou, Q. (2024). Advances in Valorization of Biomass-Derived Glycolic Acid Toward Polyglycolic Acid Production. *Catalysts*, *14*(12), 903.
- Liu, Y., Wang, L., Wang, F., & Ma, S. (2024). Preparation of interwoven structure composite paper via polylactic acid infiltrating fiber network. *Journal of Applied Polymer Science*, *141*(23), e55483.

- López de Dicastillo, C., Garrido, L., Velásquez, E., Rojas, A., & Gavara, R. (2021). Designing biodegradable and active multilayer system by assembling an electrospun polycaprolactone mat containing quercetin and nanocellulose between polylactic acid films. *Polymers*, 13(8), 1288.
- Lovely, B. (2024). *Development of cellulose-titanium dioxide-porphyrin nanocomposite films with high-barrier, UV-blocking, and visible light-responsive antimicrobial features* [Virginia Polytechnic Institute and State University]. Virginia Tech.
- Lovely, B., Kim, Y.-T., Huang, H., Zink-Sharp, A., & Roman, M. Impacts of Cycles of a Novel Low-Pressure Homogenization Process on Cellulose Nanofibrils (Cnf) as a Sustainable Packaging Film Material. *Available at SSRN 4977862*.
- Lovely, B., Kim, Y.-T., Huang, H., Zink-Sharp, A., & Roman, M. (2025). Impacts of cycles of a novel low-pressure homogenization process on cellulose nanofibrils (CNF) as a sustainable packaging film material. *Carbohydrate Polymer Technologies and Applications*, 100739.
- Low, Y. J., Andriyana, A., Ang, B. C., & Zainal Abidin, N. I. (2020). Bioresorbable and degradable behaviors of PGA: Current state and future prospects. *Polymer Engineering & Science*, 60(11), 2657-2675.
- Ma, C., Zhu, M., Gong, M., Zhang, L., Wang, D., & Lin, X. (2025). Strong, tough and aqua-degradable poly (glycolic acid)/poly (butyleneadipate-co-terephthalate) composites achieved by interfacial regulation. *Journal of Materials Research and Technology*, 35, 995-1007.
- Ma, Z., Zhao, N., & Xiong, C. (2012). Degradation and miscibility of poly (DL-lactic acid)/poly (glycolic acid) composite films: Effect of poly (DL-lactic-co-glycolic acid). *Bulletin of Materials Science*, 35, 575-578.
- Marchetti, A., Marelli, E., Bergamaschi, G., Lahtinen, P., Paananen, A., Linder, M., Pigliacelli, C., & Metrangolo, P. (2024). Nanocellulose-short peptide self-assembly for improved mechanical strength and barrier performance. *Journal of Materials Chemistry B*, 12(37), 9229-9237.
- Maxfield, F. R. (1994). Introduction: optical microscopy in physiological investigations. *FASEB Journal: Official Publication of the Federation of American Societies for Experimental Biology*, 8(9), 571-572.
- Memon, A., Ithisoponakul, S., Pramoonmak, S., Leenoi, D., & Passadee, N. (2011). A development of laminating mulberry paper by biodegradable films. *Energy Procedia*, 9, 598-604.
- Middleton, J. C., & Tipton, A. J. (2000). Synthetic biodegradable polymers as orthopedic devices. *Biomaterials*, 21(23), 2335-2346.
- Miller, K. S., & Krochta, J. (1997). Oxygen and aroma barrier properties of edible films: A review. *Trends in food science & technology*, 8(7), 228-237.
- Mirabal, A., Loza-Hernandez, I., Clark, C., Hooks, D. E., McBride, M., & Stull, J. A. (2023). Roughness measurements across topographically varied additively manufactured metal surfaces. *Additive Manufacturing*, 69, 103540.
- Mirmehdi, S., de Oliveira, M. L. C., Hein, P. R. G., Dias, M. V., Sarantópoulos, C. I. G. d. L., & Tonoli, G. H. D. (2018). Spraying cellulose nanofibrils for improvement of tensile and barrier properties of writing & printing (W&P) paper. *Journal of Wood Chemistry and Technology*, 38(3), 233-245.

- Mirmehdi, S., Hein, P. R. G., de Luca Sarantópoulos, C. I. G., Dias, M. V., & Tonoli, G. H. D. (2018). Cellulose nanofibrils/nanoclay hybrid composite as a paper coating: Effects of spray time, nanoclay content and corona discharge on barrier and mechanical properties of the coated papers. *Food Packaging and Shelf Life*, *15*, 87-94.
- Mitchell, G. R., & Tojeira, A. (2016). *Controlling the morphology of polymers: multiple scales of structure and processing*. Springer.
- Moghimi, N., Sagi, H., & Park, S.-i. (2018). Leakage analysis of flexible packaging: Establishment of a correlation between mass extraction leakage test and microbial ingress. *Food Packaging and Shelf Life*, *16*, 225-231.
- Morita, S., Takagi, T., Abe, R., Tsujimoto, H., Ozamoto, Y., Torii, H., & Hagiwara, A. (2018). Newly developed polyglycolic acid reinforcement unified with sodium alginate to prevent adhesion. *BioMed Research International*, *2018*(1), 4515949.
- Moura, A. V. d. S. (2016). Ana Sofia Lemos Machado Abreu, Isabel Gonçalves de. *Food Packaging*, 329.
- Murcia Valderrama, M. A., van Putten, R.-J., & Gruter, G.-J. M. (2020). PLGA barrier materials from CO₂. The influence of lactide co-monomer on glycolic acid polyesters. *ACS applied polymer materials*, *2*(7), 2706-2718.
- Ncube, L. K., Ude, A. U., Ogunmuyiwa, E. N., Zulkifli, R., & Beas, I. N. (2021). An overview of plastic waste generation and management in food packaging industries. *Recycling*, *6*(1), 12.
- Negro, C., Pettersson, G., Mattsson, A., Nyström, S., Sanchez-Salvador, J. L., Blanco, A., & Engstrand, P. (2023). Synergies between fibrillated nanocellulose and hot-pressing of papers obtained from high-yield pulp. *Nanomaterials*, *13*(13), 1931.
- Nerín, C., & Asensio, E. (2007). Migration of organic compounds from a multilayer plastic–paper material intended for food packaging. *Analytical and Bioanalytical Chemistry*, *389*, 589-596.
- Niu, D.-Y., Xu, P.-W., Xu, S.-J., Li, J.-X., Yang, W.-J., & Ma, P.-M. (2023). Robust poly (glycolic acid) films with crystal orientation and reinforcement of chain entanglement network. *Chinese Journal of Polymer Science*, *41*(7), 1093-1103.
- Niu, D., Xu, P., Li, J., Yang, W., Liu, T., & Ma, P. (2023). Strong, ductile and durable Poly (glycolic acid)-based films by constructing crystalline orientation, entanglement network and rigid amorphous fraction. *Polymer*, *264*, 125532.
- Pauleau, Y. (2006). *Materials surface processing by directed energy techniques*. Elsevier.
- Peng, C., Lyu, M., Guo, P., Jia, Z., Li, M., Sang, L., & Wei, Z. (2025). Toughening Biodegradable Poly (glycolic acid) with Balanced Mechanical Properties by Biobased Poly (butylene 2, 5-furanoate). *Journal of Polymers and the Environment*, 1-12.
- Peters, R., Charleston, L. A., van Eck, K., van Berlo, T., & Wilson, D. A. (2025). Hot shape transformation: the role of PSar dehydration in stomatocyte morphogenesis. *Beilstein Journal of Organic Chemistry*, *21*(1), 47-54.
- Regubalan, B., Manibalan, S., & Pandit, P. (2022). Polyglycolic acid-based bionanocomposites for food packaging applications. In *Bionanocomposites for Food Packaging Applications* (pp. 153-164). Elsevier.
- Reimer, L. (2000). Scanning electron microscopy: physics of image formation and microanalysis. *Measurement Science and Technology*, *11*(12), 1826-1826.

- Rhim, J.-W., Lee, J.-H., & Hong, S.-I. (2006). Water resistance and mechanical properties of biopolymer (alginate and soy protein) coated paperboards. *LWT-Food Science and Technology*, 39(7), 806-813.
- Rocca-Smith, J. R., Pasquarelli, R., Lagorce-Tachon, A., Rousseau, J., Fontaine, S., Aguié-Béghin, V., Debeaufort, F., & Karbowiak, T. (2019). Toward sustainable PLA-based multilayer complexes with improved barrier properties. *ACS Sustainable Chemistry & Engineering*, 7(4), 3759-3771.
- Roman, M., & Winter, W. T. (2004). Effect of sulfate groups from sulfuric acid hydrolysis on the thermal degradation behavior of bacterial cellulose. *Biomacromolecules*, 5(5), 1671-1677.
- Rosenboom, J.-G., Langer, R., & Traverso, G. (2022). Bioplastics for a circular economy. *Nature Reviews Materials*, 7(2), 117-137.
- Russo, G. M., Simon, G. P., & Incarnato, L. (2006). Correlation between rheological, mechanical, and barrier properties in new copolyamide-based nanocomposite films. *Macromolecules*, 39(11), 3855-3864.
- Samantaray, P. K., Little, A., Haddleton, D. M., McNally, T., Tan, B., Sun, Z., Huang, W., Ji, Y., & Wan, C. (2020). Poly (glycolic acid)(PGA): A versatile building block expanding high performance and sustainable bioplastic applications. *Green Chemistry*, 22(13), 4055-4081.
- Schmidt, C., Behl, M., Lendlein, A., & Beuermann, S. (2014). Synthesis of high molecular weight polyglycolide in supercritical carbon dioxide. *RSC advances*, 4(66), 35099-35105.
- Schmidt, J., Grau, L., Auer, M., Maletz, R., & Woidasky, J. (2022). Multilayer packaging in a circular economy. *Polymers*, 14(9), 1825.
- Seo, Y., & Hwang, B. (2019). Mulberry-paper-based composites for flexible electronics and energy storage devices. *Cellulose*, 26(16), 8867-8875.
- Shanmugam, K. (2022). Spray coated cellulose nanofiber laminates on the paper to enhance its barrier and mechanical properties. *Journal of Sustainability and Environmental Management*, 1(1), 10-17.
- Shanmugam, K. (2024). Application of Spray Coating in the Fabrication of Free Standing Nanocellulose Films and Barrier Coating on the Paper Substrates. *Scientific and Social Research*, 6(5), 222-245. <https://ojs.bbwpublisher.com/index.php/ssr/article/view/6207>
- Shum, A. W., & Mak, A. F. (2003). Morphological and biomechanical characterization of poly (glycolic acid) scaffolds after in vitro degradation. *Polymer Degradation and Stability*, 81(1), 141-149.
- Siracusa, V. (2012). Food packaging permeability behaviour: A report. *International Journal of Polymer Science*, 2012(1), 302029.
- Song, G., Wang, Y., & Tan, D. Q. (2022). A review of surface roughness impact on dielectric film properties. In: Wiley Online Library.
- Spence, J. C. (2013). *High-resolution electron microscopy*. OUP Oxford.
- Tamizhdurai, P., Mangesh, V., Santhosh, S., Vedavalli, R., Kavitha, C., Bhutto, J. K., Alreshidi, M. A., Yadav, K. K., & Kumaran, R. (2024). A state-of-the-art review of multilayer packaging recycling: Challenges, alternatives, and outlook. *Journal of Cleaner Production*, 141403.

- Tang, S., Zhang, R., Liu, F., & Liu, X. (2015). Hansen solubility parameters of polyglycolic acid and interaction parameters between polyglycolic acid and solvents. *European Polymer Journal*, *72*, 83-88.
- Tanpichai, S., Srimarut, Y., Woraprayote, W., & Malila, Y. (2022). Chitosan coating for the preparation of multilayer coated paper for food-contact packaging: Wettability, mechanical properties, and overall migration. *International journal of biological macromolecules*, *213*, 534-545.
- Torun, I., & Onses, M. S. (2017). Robust superhydrophobicity on paper: Protection of spray-coated nanoparticles against mechanical wear by the microstructure of paper. *Surface and Coatings Technology*, *319*, 301-308.
- Twede, D., Selke, S. E., Kamdem, D.-P., & Shires, D. (2014). *Cartons, crates and corrugated board: handbook of paper and wood packaging technology*. DEStech Publications, Inc.
- Vargha-Butler, E., Kiss, E., Lam, C., Keresztes, Z., Kálmán, E., Zhang, L., & Neumann, A. (2001). Wettability of biodegradable surfaces. *Colloid and Polymer Science*, *279*, 1160-1168.
- Vartiainen, J., Lahtinen, P., Kaljunen, T., Kunnari, V., Peresin, M. S., & Tammelin, T. (2015). Comparison of properties between cellulose nanofibrils made from banana, sugar beet, hemp, softwood and hardwood pulps. *O Pap*, *76*(3), 1.
- Vartiainen, J., Shen, Y., Kaljunen, T., Malm, T., Vähä-Nissi, M., Putkonen, M., & Harlin, A. (2016). Bio-based multilayer barrier films by extrusion, dispersion coating and atomic layer deposition. *Journal of Applied Polymer Science*, *133*(2).
- Vieira, M. G. A., Da Silva, M. A., Dos Santos, L. O., & Beppu, M. M. (2011). Natural-based plasticizers and biopolymer films: A review. *European Polymer Journal*, *47*(3), 254-263.
- Vinet, L., & Zhedanov, A. (2011). A 'missing' family of classical orthogonal polynomials. *Journal of Physics A: Mathematical and Theoretical*, *44*(8), 085201.
- Wang, F.-j., Wang, L.-q., Zhang, X.-c., Ma, S.-f., & Zhao, Z.-c. (2022). Study on the barrier properties and antibacterial properties of cellulose-based multilayer coated paperboard used for fast food packaging. *Food Bioscience*, *46*, 101398.
- Wang, J., Gardner, D. J., Stark, N. M., Bousfield, D. W., Tajvidi, M., & Cai, Z. (2018). Moisture and oxygen barrier properties of cellulose nanomaterial-based films. *ACS Sustainable Chemistry & Engineering*, *6*(1), 49-70.
- Wang, L., Chen, C., Wang, J., Gardner, D. J., & Tajvidi, M. (2020). Cellulose nanofibrils versus cellulose nanocrystals: Comparison of performance in flexible multilayer films for packaging applications. *Food Packaging and Shelf Life*, *23*, 100464.
- Wei, L., Ma, S., Hao, M., Ma, L., & Lin, X. (2022). Modifying Anti-Compression Property and Water-Soluble Ability of Polyglycolic Acid via Melt Blending with Polyvinyl Alcohol. *Polymers*, *14*(16), 3375.
- Woch, J., Małachowska, E., Korasiak, K., Lipkiewicz, A., Dubowik, M., Chrobak, J., Iłowska, J., & Przybysz, P. (2022). Barrier dispersion-based coatings containing natural and paraffin waxes. *Molecules*, *27*(3), 930.
- Wolf, F. K., Fischer, A. M., & Frey, H. (2010). Poly (glycolide) multi-arm star polymers: Improved solubility via limited arm length. *Beilstein Journal of Organic Chemistry*, *6*(1), 0-0.

- Yang, B., Zhang, M., Lu, Z., Tan, J., Luo, J., Song, S., Ding, X., Wang, L., Lu, P., & Zhang, Q. (2019). Comparative study of aramid nanofiber (ANF) and cellulose nanofiber (CNF). *Carbohydrate polymers*, 208, 372-381.
- Yang, P., Wu, H., Yang, F., Yang, J., Wang, R., & Zhu, Z. (2021). A novel self-assembled graphene-based flame retardant: synthesis and flame retardant performance in PLA. *Polymers*, 13(23), 4216.
- Yoon, S. K., Yang, J. H., Lim, H. T., Chang, Y.-W., Ayyoob, M., Yang, X., Kim, Y. J., Ko, H.-S., Jho, J. Y., & Chung, D. J. (2020). In vitro and in vivo biosafety analysis of resorbable polyglycolic acid-poly(lactic acid) block copolymer composites for spinal fixation. *Polymers*, 13(1), 29.
- Yu, C., Bao, J., Xie, Q., Shan, G., Bao, Y., & Pan, P. (2016). Crystallization behavior and crystalline structural changes of poly (glycolic acid) investigated via temperature-variable WAXD and FTIR analysis. *CrystEngComm*, 18(40), 7894-7902.
- Yuan, Q., Wu, J., Qin, C., Xu, A., Zhang, Z., Lin, S., Ren, X., & Zhang, P. (2016). Spin-coating synthesis and characterization of Zn-doped hydroxyapatite/poly(lactic acid) composite coatings. *Surface and Coatings Technology*, 307, 461-469.
- Zhang, J., Xu, B., Zhang, P., Cai, M., & Li, B. (2023). Effects of surface roughness on wettability and surface energy of coal. *Frontiers in Earth Science*, 10, 1054896.

Supplemental Data

Scanning Electron Microscopy (SEM)

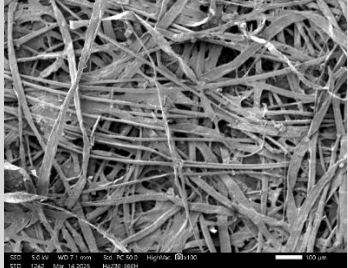
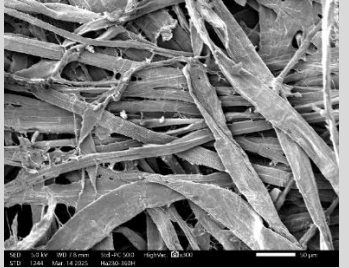
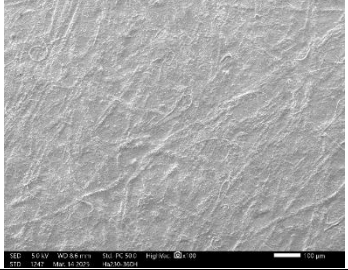
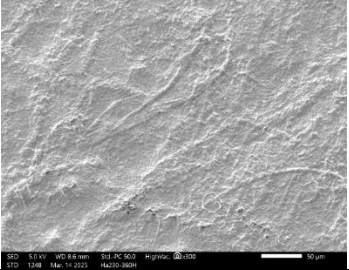
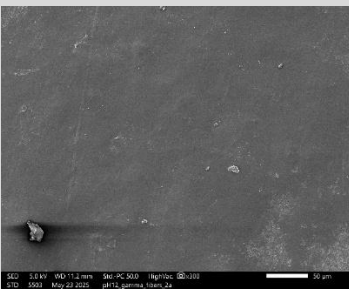
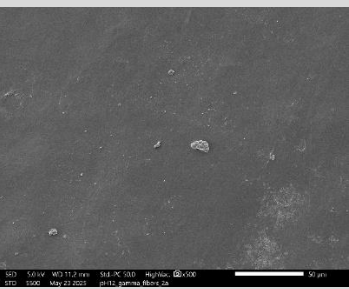
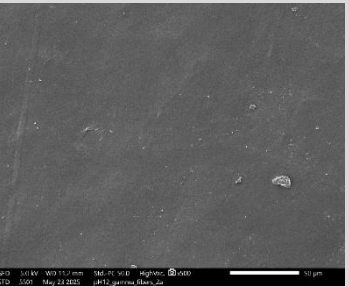
	100 X	300 X	500 X
Paper			N/A
Paper/CNF-5			N/A
Paper/CNF-5/PGA	N/A		
	N/A	N/A	

Figure S1. SEM surface morphology of the dual-layer packaging samples.

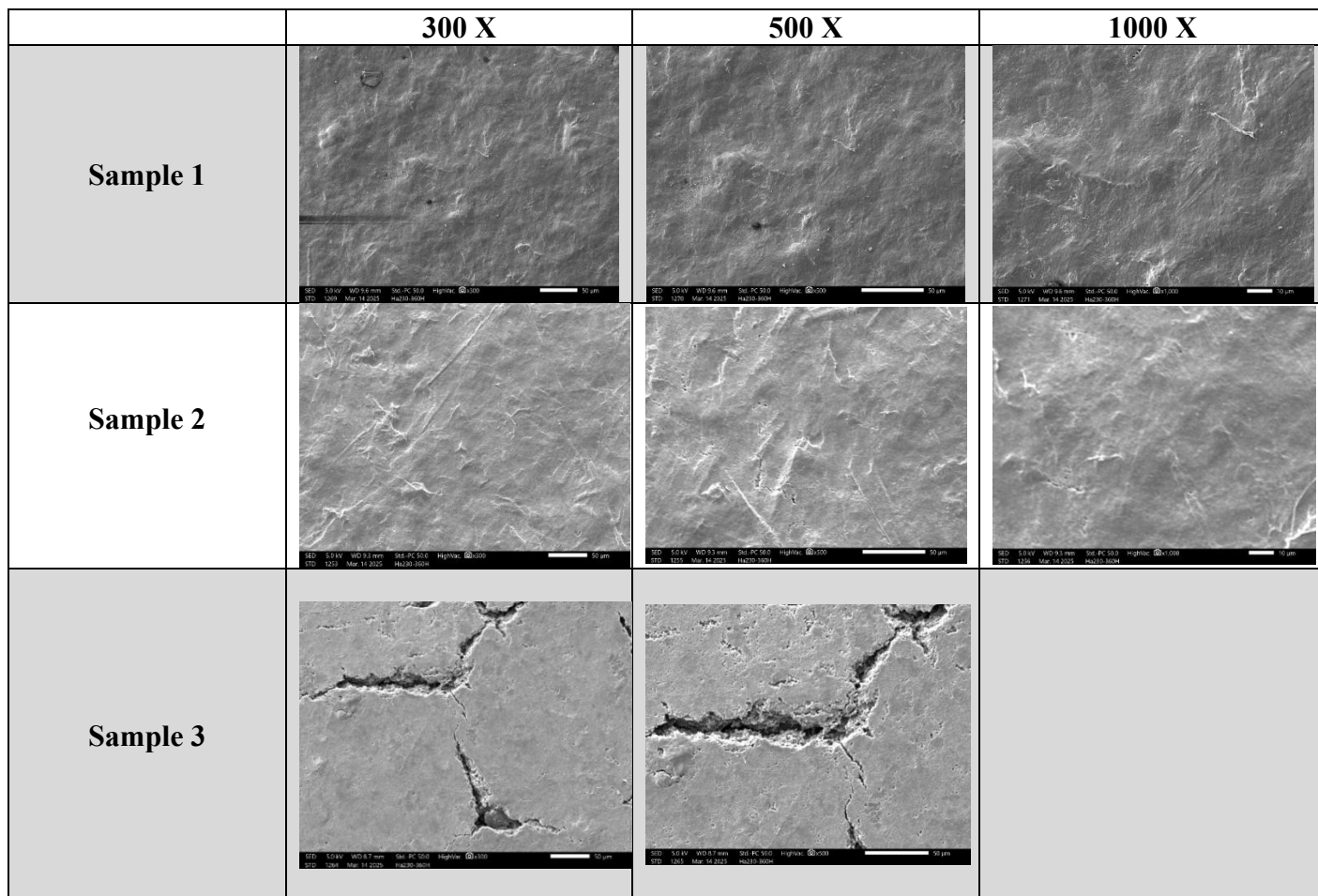
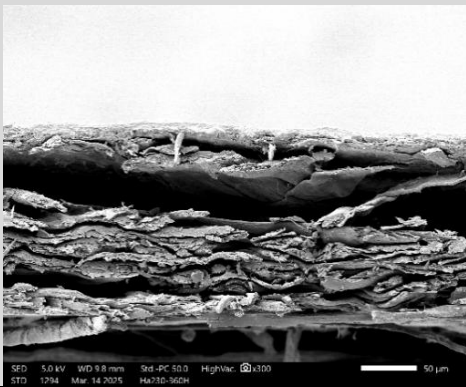
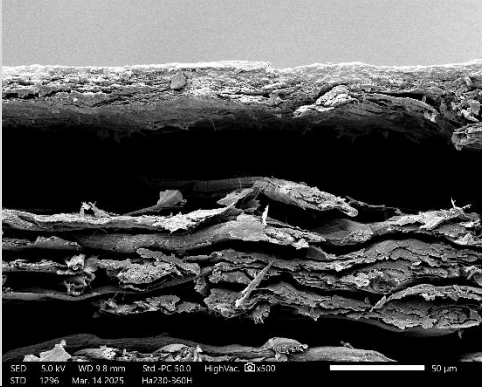
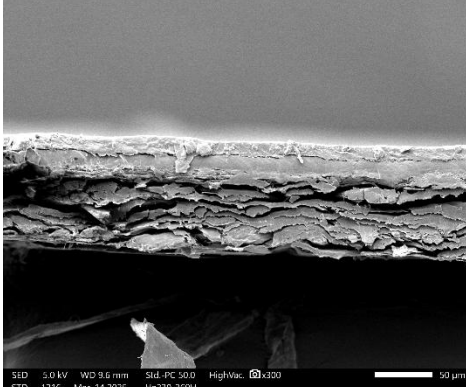
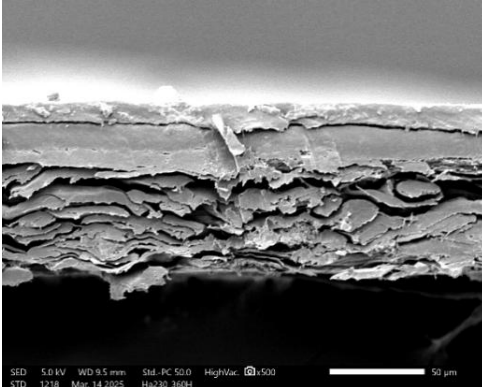
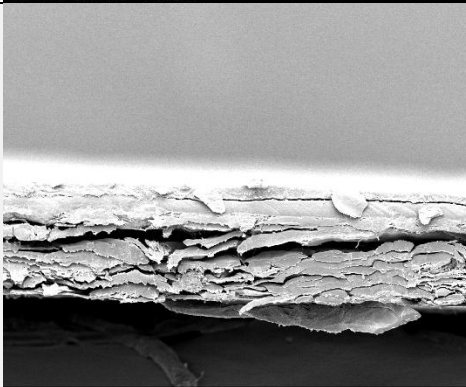
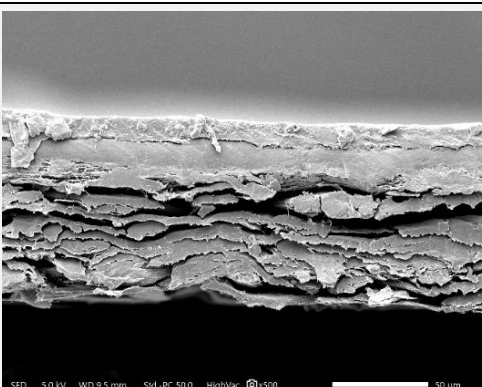
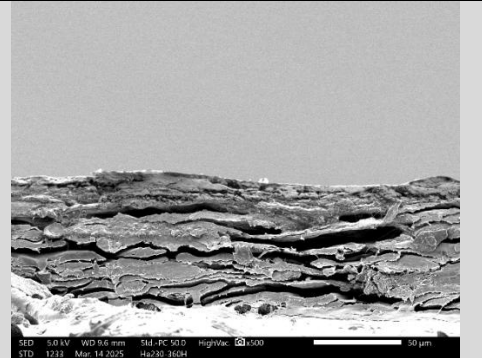


Figure S2. SEM surface morphology of Paper/CNF-5/PGA samples without plasticizers.

	300 X	500 X
Sample 1	 <p>SED 5.0 kV WD 9.8 mm Std.-PC 50.0 HighVac x300 STD 1294 Mar 14 2025 Ha230-360H 50 µm</p>	 <p>SED 5.0 kV WD 9.8 mm Std.-PC 50.0 HighVac x500 STD 1296 Mar 14 2025 Ha230-360H 50 µm</p>
Sample 2	 <p>SED 5.0 kV WD 9.6 mm Std.-PC 50.0 HighVac x300 STD 1216 Mar 14 2025 Ha230-360H 50 µm</p>	 <p>SED 5.0 kV WD 9.5 mm Std.-PC 50.0 HighVac x500 STD 1218 Mar 14 2025 Ha230-360H 50 µm</p>
	 <p>SED 5.0 kV WD 9.6 mm Std.-PC 50.0 HighVac x300 STD 1215 Mar 14 2025 Ha230-360H 50 µm</p>	 <p>SED 5.0 kV WD 9.5 mm Std.-PC 50.0 HighVac x500 STD 1217 Mar 14 2025 Ha230-360H 50 µm</p>
Sample 4	N/A	 <p>SED 5.0 kV WD 9.6 mm Std.-PC 50.0 HighVac x500 STD 1233 Mar 14 2025 Ha230-360H 50 µm</p>

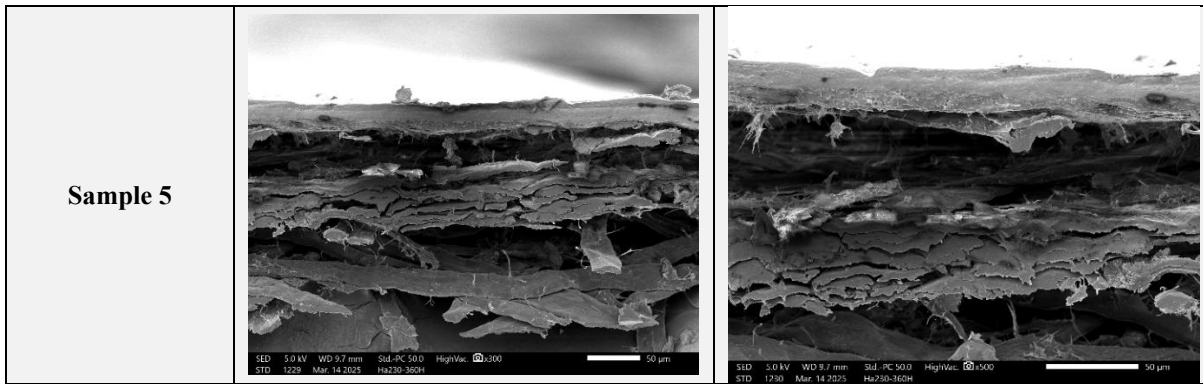


Figure S3. SEM cross-sectional morphology of Paper/CNF-5/PGA samples without plasticizers.

Surface Roughness

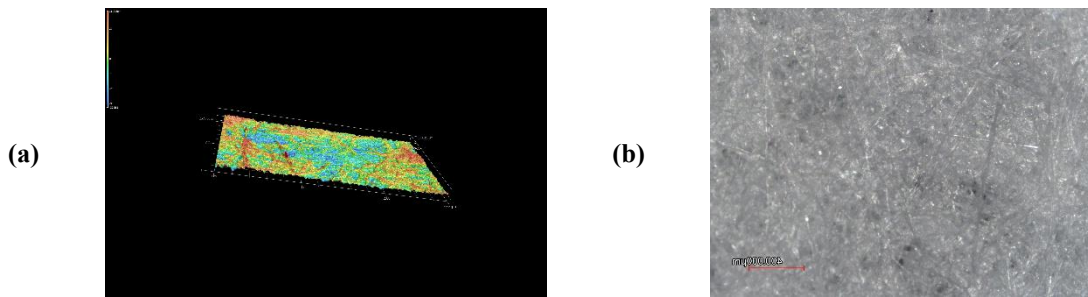


Figure S4. Surface roughness of unpressed mulberry fiber paper (a) 3D and (b) z-stack images.

Table S1. Surface roughness of unpressed mulberry fiber paper: arithmetical mean height or S_a

Samples	S_a (μm)
Paper	9.73 ± 1.24